



# A spectral approach for fuzzy uncertainty propagation in finite element analysis

S. Adhikari<sup>\*</sup>, H. Haddad Khodaparast

*College of Engineering, Swansea University, Singleton Park, Swansea SA2 8PP, UK*

Received 13 November 2011; received in revised form 8 October 2013; accepted 9 October 2013

Available online 16 October 2013

---

## Abstract

Uncertainty propagation in complex engineering systems with fuzzy variables constitutes a significant challenge. This paper proposes a Polynomial Chaos type spectral approach based on orthogonal function expansion. A fuzzy variable is represented as a set of interval variables via the membership function. The interval variables are further transformed into the standard interval  $[-1, 1]$ . Smooth nonlinear functions of standard interval variables are projected in the basis of Legendre polynomials by exploiting its orthogonal properties over the interval  $[-1, 1]$ . The coefficients associated with the basis functions are obtained by a Galerkin type of error minimisation. The method is first illustrated using scalar functions of multiple fuzzy variables. Later the method is proposed for elliptic type finite element problems where the technique is extended to vector valued functions with multiple fuzzy variables. The response of such systems can be expressed in the complete basis of multivariate Legendre polynomials. The coefficients, obtained by Galerkin type of error minimisation, can be calculated from the solution of an extended set of linear algebraic equations. An eigenfunction based model reduction technique is proposed to obtain the coefficient vectors in an efficient way. A numerical example of axial deformation of a rod with fuzzy axial stiffness is considered to illustrate the proposed methods. Linear and nonlinear membership functions are used and the results are compared with direct numerical simulation results.

© 2013 Elsevier B.V. All rights reserved.

*Keywords:* Fuzzy systems; Structural mechanics; Uncertainty propagation; Polynomial chaos; Spectral approach

---

## 1. Introduction

Finite element method [1] has been used widely for numerical simulation of complex engineering systems. The consideration of uncertainties in numerical models to obtain the variability of response is becoming more common for finite element models arising in practical problems. When substantial statistical information exists, the theory of probability and stochastic processes offer a rich mathematical framework to represent such uncertainties. In a probabilistic setting, uncertainty associated with the system parameters, such as the geometric properties and constitutive relations (i.e. Young's modulus, mass density, Poisson's ratio, damping coefficients), can be modeled as random variables or stochastic processes using the so-called parametric approach. These uncertainties can be quantified and propagated, for example, using the stochastic finite element method [2–4]. The reliable application of probabilistic approaches

---

<sup>\*</sup> Corresponding author. Tel.: +44 (0)1792 602088; fax: +44 (0)1792 295676.  
E-mail address: [S.Adhikari@swansea.ac.uk](mailto:S.Adhikari@swansea.ac.uk) (S. Adhikari).

requires information to construct the probability density functions of uncertain parameters. This information may not be easily available for many complex practical problems. In such situations, non-probabilistic approaches such as interval algebra [5], convex models [6] and fuzzy set [7] based methods can be used. In this paper the uncertain variables describing the system parameters are modeled using fuzzy variables.

Fuzzy finite element analysis (see for example the review papers [8–10]) aims to combine the power of finite element method and uncertainty modelling capability of fuzzy variables. One way to view a fuzzy variable is the generalisation of an interval variable. It should be noted that the intervals do not represent the values of the variable, but our knowledge about the range of possible values the variable can take. When an uncertain variable is modelled using the interval approach, the values of the variable lie within a lower and an upper bound. The fuzzy approach generalises this concept by introducing a membership function. In the context of computational mechanics, the aim of a fuzzy finite element analysis is to obtain the membership function of the output quantities (such as displacement, acceleration and stress) given the membership of data in the set of input variables. This problem, known as the uncertainty propagation problem, has taken the centre stage in recent research activities in the field. In principle an uncertainty propagation problem can be always solved using the so-called direct Monte Carlo simulation. Using this approach, a large number of members of the parameter set are individually simulated and bounds are obtained from the resulting outputs. For the most practical problems, direct Monte Carlo simulation is prohibitively computationally expensive. Therefore, the aim of the majority of current research is to reduce the computational cost. Under the possibilistic interpretation of fuzzy sets and using the min-operator as t-norm [11,12], fuzzy variables would become a generalisation of interval variables. Consequently methods applicable for interval analysis such as classical interval arithmetic [5], affine analysis [13] or vertex theorems [14] can be used. The Neumann expansion [15], the transformation method [16], and more recently, response surface based methods [17] have been proposed for fuzzy uncertainty propagation. In the context of structural dynamical systems, several authors have extended the classical modal analysis to fuzzy modal analysis [18–22]. Fuzzy approach has been applied to safety analysis [23,24], optimal design [25] and also boundary element analysis [26]. Recently a High Dimensional Model Representation (HDMR) approach has been proposed [27] for the propagation of fuzzy uncertain variables through a complex finite element model.

In spite of these significant developments in the methodology of fuzzy uncertainty propagation through complex systems, probabilistic uncertainty propagation methodologies perhaps still have the edge due to the availability of a wide-ranging techniques suited for various problems. Among the various available methods, the spectral methods [2] have received considerable attention [28]. These methods, generally known as polynomial chaos [29], stand on rigorous mathematical footing and provide a practical computational approach which is general enough to be used within the context of finite element method for complex systems [2]. Although the probabilistic approaches are powerful tools for reliability analysis in structural engineering design [30], these approaches usually require large volumes of data. However when limited information is available, the probabilistic approaches lose their performance significantly and might not be reliable to be used on their own. Fuzzy methods are found to have a better performance compared to probabilistic approaches in the face of lack of information [31]. Therefore, using a mixture of different uncertainty models in complex engineering systems may be useful, as neither the fuzzy description nor the probabilistic description may be available for *all* the uncertain parameters. Currently different mathematical techniques are being used for fuzzy and probabilistic variables. In this paper we propose a new technique by which spectral methods originally introduced for probabilistic uncertainty propagation, can be extended for fuzzy uncertainty propagation with suitable adaptations. The main motivation behind this work arises from computational efficiency, generality and rigour behind the fuzzy uncertainty propagation technique and also having a synergy between probabilistic and fuzzy approaches. Such synergy in the propagation technique between different uncertainty modelling approaches may lead to unified approaches whereby different types of uncertainty can be mathematically handled simultaneously in a consistent manner. Our approach relies on the decomposition of a fuzzy variable into parameterised interval variables and projecting the response function of these variables into a complete orthonormal basis of polynomial functions. The coefficients associated with the basis functions are obtained by a Galerkin type of error minimisation.

The outline of the paper is as follows. Section 2 gives a brief background of fuzzy variables. Legendre polynomials and its application for propagation of fuzzy variables through general nonlinear scalar functions are discussed in Section 3. Two simple numerical examples are given to illustrate the idea behind the proposed spectral approach. In Section 4 spectral finite element analysis with fuzzy variables for elliptic problems is proposed. A reduced computational approach is proposed in Section 4.3. A numerical example of axial deformation of a rod with fuzzy axial stiffness is given in Section 5 to illustrate the proposed methods. Different types of membership functions are used

and the results are compared with direct numerical simulation results. Conclusions are drawn in Section 6 based on theoretical and numeral results obtained in the paper.

## 2. A brief overview of fuzzy variables

In this section, we provide a brief description of fuzzy variables and refer the reader to established books [32–34] and relevant review papers [8,9] for more details. The fuzzy set is generally defined by its membership function. The membership function of a fuzzy set can be interpreted as a distribution of uncertainty [35], which was proposed by Zadeh [36]. In this interpretation, the membership function indicates the degree of possibility that an element belongs to a given fuzzy set. In other words, it represents the possibility distribution of some uncertain variable and can be considered as an alternative to the probability distribution. For a normal fuzzy set, the membership value varies within the range of 0 to 1. Membership value of one ( $\mu_{\tilde{A}}(x) = 1$ ) indicates that the element  $x$  belongs to the fuzzy set  $\tilde{A}$ . On the other hand, if  $\mu_{\tilde{A}}(x) = 0$  then  $x$  is definitely not a member of the fuzzy set  $\tilde{A}$ . For any intermediate case  $0 < \mu_{\tilde{A}}(x) < 1$  the membership is gradual. Therefore, an one-dimensional fuzzy set  $\tilde{A}$  can be expressed by a set of pairs consisting of the elements  $x \in \mathbb{R}$  and their corresponding membership function value  $\mu_{\tilde{A}}(x)$ :

$$\tilde{A} = \{(x, \mu_{\tilde{A}}(x)) \mid x \in \mathbb{R}, \mu_{\tilde{A}}(x) \in [0, 1]\} \tag{1}$$

In the multidimensional case, an  $n$ -array fuzzy relation  $\tilde{\mathbf{A}}$  is defined as a set of pairs which consist of vector  $\mathbf{x} \in \mathbb{R}^m$  and their corresponding membership functions  $\mu_{\tilde{\mathbf{A}}}(\mathbf{x})$ :

$$\tilde{\mathbf{A}} = \{(\mathbf{x}, \mu_{\tilde{\mathbf{A}}}(\mathbf{x})) \mid \mathbf{x} \in \mathbb{R}^m, \mu_{\tilde{\mathbf{A}}}(\mathbf{x}) \in [0, 1]\} \tag{2}$$

In this paper only normalised fuzzy sets are considered and therefore  $\sup_{x \in \mathbb{R}} \mu_{\tilde{A}}(x) = 1$ . The fuzzy set is said to be non-interactive fuzzy set if the components of vector  $\mathbf{x} = [x_1, x_2, \dots, x_m]$  in Eq. (2) are independent. The non-interactive fuzzy set is used in this paper. Therefore the definition in Eq. (2) can be described as Cartesian product of  $m$  one-dimensional fuzzy set  $\tilde{\mathbf{A}} = [\tilde{A}_1, \tilde{A}_2, \dots, \tilde{A}_m]$  where each component has the same definition given in Eq. (1). Based on possibility theory [11,12],  $\alpha$ -cuts of a possibility distribution correspond to confidence intervals of degree  $(1 - \alpha)$  [37]. The locations of intervals obtained by  $\alpha$ -cuts can then specify the possibility distribution of an uncertain parameter. In this context, the notion of support and  $\alpha$ -cuts [18,38,39] of a fuzzy set plays a crucial role in the computational and analytical methods involving fuzzy sets. The support of a fuzzy set  $\tilde{A}$  is the crisp set of all  $x \in \mathbb{R}$ , such that  $\mu_{\tilde{A}}(x) > 0$ , or mathematically

$$\text{supp}(\tilde{A}) = \{x \mid \mu_{\tilde{A}}(x) > 0, x \in \mathbb{R}\} \tag{3}$$

The  $\alpha$ -cut or  $\alpha$ -level set of  $\tilde{A}$  is the crisp set  $A_\alpha$  such that

$$A_\alpha = \{x \mid \mu_{\tilde{A}}(x) \geq \alpha, x \in \mathbb{R}, 0 < \alpha \leq 1\} \tag{4}$$

The crisp set  $A_\alpha$  is an interval variable  $x_\alpha^I$  resulting from intersecting the membership function at  $\mu_{\tilde{A}}(x_i) = \alpha$  and mathematically defined as

$$x_\alpha^I = [\underline{x}^{(\alpha)}, \bar{x}^{(\alpha)}] = \{x \in \mathbb{R} \mid \underline{x}^{(\alpha)} \leq x \leq \bar{x}^{(\alpha)}\} \tag{5}$$

where  $\underline{\bullet}$  and  $\bar{\bullet}$  represent the lower and upper bounds of  $\bullet$  respectively. The propagation of fuzzy numbers/variables through numerical models is carried out level-wise, i.e. interval analysis at each  $\alpha$ -cuts. In this case, the  $\alpha$ -cuts of a fuzzy vector are defined as

$$x_{i,\alpha}^I = [\underline{x}_i^{(\alpha)}, \bar{x}_i^{(\alpha)}] = \{x_i^{(\alpha)} \in \mathbb{R} \mid \mu_{\tilde{A}_i}(x_i) \geq \alpha\} \tag{6}$$

where  $i = 1, 2, \dots, m$  and the fuzzy analysis involves the application of interval analysis at a number of  $\alpha$ -levels. Another important property of the fuzzy set is the convexity. In general, a fuzzy set is convex if and only if all possible  $\alpha$ -cuts of the set are convex in the classical set theoretical sense [32]. The mathematical definition of a convex fuzzy set is

$$\lambda u + (1 - \lambda)v \in A_\alpha, \quad \forall \lambda \in [0, 1] \tag{7}$$

where  $u \in A_\alpha$  and  $v \in A_\alpha$  are the elements that belong to the alpha-cut crisp set ( $A_\alpha$ ). Finally the compact fuzzy set is defined.  $\tilde{A}$  is compact if its support is bounded. It should be noted that, in the case of bounded supports, we also define the 0-cut as the largest closed interval  $A_0 = [\inf(\text{supp}(\tilde{A})), \sup(\text{supp}(\tilde{A}))]$ . Sometimes  $\alpha$ -cuts are considered as intervals of confidence (with degree of confidence  $1 - \alpha$ ), since in case of convex fuzzy sets, they are closed intervals associated with a gradation of confidence between  $[0, 1]$ . In this paper fuzzy numbers are used. Fuzzy numbers are fuzzy sets which are normal, convex and compact and also their membership function is continuous.

### 3. Legendre polynomials for fuzzy uncertainty propagation

#### 3.1. Problem description

We are interested to obtain the membership functions of the output quantities given the membership functions of the input quantities. This can be also viewed as the propagation of an  $m$ -dimensional vector of fuzzy input variables ( $\tilde{\mathbf{x}}$ ), which can be expressed as

$$\tilde{\mathbf{y}} = \mathbf{f}(\tilde{\mathbf{x}}) \quad (8)$$

where  $\tilde{\mathbf{y}}$  is  $n$ -dimensional vector of fuzzy output variables which can be obtained from the crisp function  $\mathbf{f}(\mathbf{x}) : \mathbb{R}^m \rightarrow \mathbb{R}^n$  applied to  $m$  fuzzy input variables  $\tilde{\mathbf{x}}$ . The function  $\mathbf{f}(\bullet)$  depends on the physical problem in consideration. We are mainly interested in complex engineering mechanics problems. Zadeh's extension principle [40] gives the meaning of Eq. (8). However, the expression of the extension principle cannot be readily implemented in a numerical context. It can be proved that the extension principle is equivalent to interval analysis on  $\alpha$ -cuts [41]. Based on this view, the solution is to search in the output domain for sets that have an equal degree of membership function. Therefore, fuzzy uncertainty propagation involves the application of a numerical procedure of interval analysis at a number of  $\alpha$ -levels. There are two approaches for uncertainty propagation of fuzzy variables through smooth nonlinear functions. The first approach is known as the *Interval algebra based approach*. In this approach a fuzzy variable is considered as an interval variable for each  $\alpha$ -cut and propagated using classical interval arithmetic [5]. However, it is reported in the literature that interval algebra method provides conservative bounds of the outputs mainly due to neglecting the correlation between the operands (see for example [8]). In spite of the available approaches [42] that aimed at overcoming the issues with interval algebra method and the applicability of the method to certain engineering problems (e.g. [39]), it is still not a recommended approach. The second approach, which is more commonly used in the complex engineering mechanics problem, is known as the *Global optimisation based approach* [10]. Here for each  $\alpha$ -cut two optimisation problems are solved for each of the output quantities. The first optimisation problem aims to find the minimum value while the second optimisation problem aims to find the maximum value of the output quantity. By combining results for all  $\alpha$ -cuts, one can obtain the fuzzy description of the output quantities. The advantage of this approach is that the bounds are 'tight' and the wealth of tools are available for mathematical optimisation can be employed in a reasonably straightforward manner. The disadvantage is, of course, the computational cost as two optimisation problems need to be solved for every  $\alpha$ -cut and for every output quantity. For these reasons efficient numerical methods are necessary to use this approach.

The main idea proposed here is based on the efficient and accurate construction of a 'response surface' for every  $\alpha$ -cut followed by an optimisation approach. Suppose  $\mathbb{N}$  is the set of integers and  $r \in \mathbb{N}$  is the number of  $\alpha$ -cuts used for each of the input fuzzy variables  $\tilde{x}_j$ ,  $j = 1, 2, \dots, m$ , in the numerical analysis. Therefore,  $0 \leq [\alpha_1, \alpha_2, \dots, \alpha_r] < 1$  are the values of  $\alpha$  for which we wish to obtain our outputs. It should be noted that the assumption of  $\alpha_k < 1$  is due to the fact that the core of fuzzy numbers is a singleton set. Suppose the relationship between the input parameters  $\mathbf{x}^{(\alpha)}$  and the  $j$ th response vector component at  $\alpha = \alpha_k$ -level is represented by the function  $f_j^{(\alpha)}(\mathbf{x}^{(\alpha)})$ ,  $j = 1, 2, \dots, n$ ;  $\alpha = \alpha_k$ ,  $k = 1, 2, \dots, r$ . (Note that the subscript  $k$  is omitted from  $\alpha_k$  for reason of simplicity.) The range of the response vector components, represented by the lower bound  $y_j^{(\alpha)}$  and the upper bound  $\bar{y}_j^{(\alpha)}$ , on a specific level of membership function  $\alpha = \alpha_k$  is searched within the same  $\alpha$ -level on the input domain, which means the analysis at each  $\alpha$ -cut corresponds to an interval analysis for the system. The interval analysis at each  $\alpha$ -level is then a numerical procedure equivalent to solving the following set of optimisation problems:

$$\left. \begin{aligned} y_j^{(\alpha)} &= \min_{\mathbf{x}^{(\alpha)} \in \mathbf{x}_\alpha^I} f_j^{(\alpha)}(\mathbf{x}^{(\alpha)}) \\ \bar{y}_j^{(\alpha)} &= \max_{\mathbf{x}^{(\alpha)} \in \mathbf{x}_\alpha^I} f_j^{(\alpha)}(\mathbf{x}^{(\alpha)}) \end{aligned} \right\} \quad \forall j = 1, 2, \dots, n; \quad \alpha = \alpha_k, \quad k = 1, 2, \dots, r \quad (9)$$

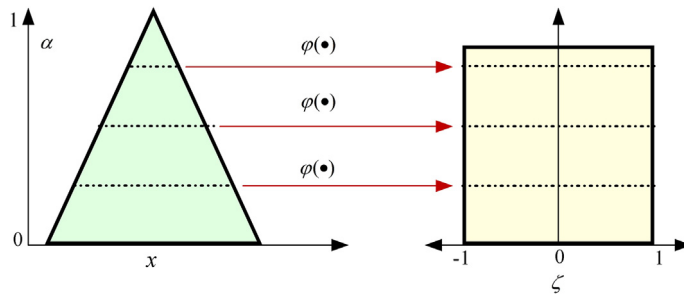


Fig. 1. Transformation of a fuzzy variable  $x$  to  $\zeta \in [-1, 1]$  for different  $\alpha$ -cuts. The transformation  $\varphi(\bullet)$  maps the interval  $[\underline{x}^{(\alpha)}, \bar{x}^{(\alpha)}] \rightarrow [-1, 1]$  where  $\alpha = \alpha_k$  and  $k = 1, 2, \dots, r$ .

In total there are  $2nr$  optimisation problems. The computational cost of each of these optimisation problems depends on the dimensionality of the  $\mathbf{x}_{\alpha_k}$  that is  $m$ . Suppose  $c(m)$  is the computational cost associated with each optimisation problem. For example, if  $f_j(\bullet)$  are monotonic functions, then the optimal values occur at the vertices of the  $m$ -dimensional parallelepiped. For this case one has  $c(m) \propto 2^m$ . Computational cost can be reduced by reducing the cost of each function evaluation, for example, by ‘replacing’ the expensive function by a surrogate model.

Recently a High Dimensional Model Representation (HDMR) approach [27] was proposed to efficiently generate a surrogate model. Here we propose an approach based on projecting the function in a basis consisting of orthogonal polynomials. The first step is to transform each interval for a given  $\alpha$ -cut ( $\alpha = \alpha_k$ ) to the space  $[-1, 1]$ . This process is depicted in Fig. 1. Suppose the transformation  $\varphi(\bullet)$  maps the interval  $[\underline{x}_i^{(\alpha)}, \bar{x}_i^{(\alpha)}] \rightarrow [-1, 1]$  where  $i$  denotes the  $i$ th input vector component. Here  $\underline{x}_i^{(\alpha)}$  and  $\bar{x}_i^{(\alpha)}$  denote the lower and upper bounds of the fuzzy variable  $\tilde{x}_i$  for a given  $\alpha$ -cut ( $\alpha = \alpha_k$ ). Denote  $\zeta_i$  as the variable bounded between  $[-1, 1]$ . Therefore, considering the variable  $x_i^{(\alpha)}$  lies between  $[\underline{x}_i^{(\alpha)}, \bar{x}_i^{(\alpha)}]$ , the linear transformation  $\varphi(\bullet)$  can be identified as

$$\zeta_i = \varphi(x_i^{(\alpha)}) = 2 \left\{ \frac{(x_i^{(\alpha)} - \underline{x}_i^{(\alpha)})}{(\bar{x}_i^{(\alpha)} - \underline{x}_i^{(\alpha)})} - \frac{1}{2} \right\} \tag{10}$$

The inverse transformation of (10) can be obtained as

$$x_i^{(\alpha)} = \left( \frac{\bar{x}_i^{(\alpha)} - \underline{x}_i^{(\alpha)}}{2} \right) \zeta_i + \frac{(\bar{x}_i^{(\alpha)} + \underline{x}_i^{(\alpha)})}{2} \tag{11}$$

Substituting  $x_i^{(\alpha)}$  in Eq. (8) for all  $\alpha = \alpha_k, k = 1, 2, \dots, r$  and  $i = 1, 2, \dots, m$ , we can formally express the uncertainty propagation problem in terms of the vector valued variable  $\boldsymbol{\zeta} = \{\zeta_i\}_{i=1, \dots, m} \in [-1, 1]^m$  as

$$\mathbf{y}^{(\alpha)} = \mathbf{f}^{(\alpha)}(\boldsymbol{\zeta}) \in \mathbb{R}^n \tag{12}$$

Next we utilise the orthogonal property of Legendre polynomials in  $[-1, 1]$  for this uncertainty propagation problem.

### 3.2. Legendre polynomials

The idea of using orthogonal functions to represent a general nonlinear function in a given domain is classical. In the context of deterministic functions, one of the earliest example is the Fourier series where sine and cosine functions are used. In the context of functions of random variables, Karhunen–Loève [2] expansion, and Polynomial Chaos expansion [2] based on original work of Wiener [29], have been extensively used. The approach taken here is motivated by the Polynomial Chaos expansion for function of random variables. First consider the special case when  $\boldsymbol{\zeta}$  is scalar, that is  $\zeta \in [-1, 1]$ . The notation denoting the dependence of  $\alpha$  is omitted for notational convenience. It is known that the Legendre polynomials are orthogonal with respect to the  $\mathcal{L}_2$  inner product norm, that is,

$$\int_{-1}^1 L_j(\zeta)L_k(\zeta) d\zeta = \frac{2}{2k + 1} \delta_{jk} \tag{13}$$

Table 1  
One dimensional Legendre polynomials upto order 10.

$k$	Legendre polynomials of order $k$ : $L_k(\zeta)$ ; $\zeta \in [-1, 1]$
0	1
1	$\zeta$
2	$\frac{1}{2}(3\zeta^2 - 1)$
3	$\frac{1}{2}(5\zeta^3 - 3\zeta)$
4	$\frac{1}{8}(35\zeta^4 - 15\zeta^2 + 3)$
5	$\frac{1}{8}(63\zeta^5 - 70\zeta^3 + 15\zeta)$
6	$\frac{1}{16}(231\zeta^6 - 315\zeta^4 + 105\zeta^2 - 5)$
7	$\frac{1}{16}(429\zeta^7 - 693\zeta^5 + 325\zeta^3 - 35\zeta)$
8	$\frac{1}{128}(6435\zeta^8 - 12012\zeta^6 + 6930\zeta^4 - 1260\zeta^2 + 35)$
9	$\frac{1}{128}(12155\zeta^9 - 25740\zeta^7 + 18018\zeta^5 - 4620\zeta^3 + 315\zeta)$
10	$\frac{1}{256}(46189\zeta^{10} - 109395\zeta^8 + 90090\zeta^6 - 30030\zeta^4 + 3465\zeta^2 - 63)$

where  $\delta_{jk}$  denotes the Kronecker delta (equal to 1 if  $j = k$  and to 0 otherwise) and  $L_j(\zeta)$  is the  $j$ th order Legendre polynomial. Legendre polynomials [43] are solution to the Legendre's differential equation

$$\frac{d}{d\zeta} \left\{ (1 - \zeta^2) \frac{d}{d\zeta} L_k(\zeta) \right\} + k(k+1)L_k(\zeta) = 0; \quad k = 0, 1, 2, \dots \quad (14)$$

The solution to this equation is convergent only between  $-1$  to  $1$ . Each Legendre polynomial  $L_j(\zeta)$  is an  $k$ th-degree polynomial and can be expressed using Rodrigues' formula as

$$L_k(\zeta) = \frac{1}{2^k k!} \frac{d^k}{d\zeta^k} \{ (1 - \zeta^2)^k \}; \quad k = 0, 1, 2, \dots \quad (15)$$

Legendre polynomials of any order can also be conveniently expressed by a recursive relationship as

$$L_0(\zeta) = 1, \quad L_1(\zeta) = \zeta \quad (16)$$

$$L_{k+1} = \frac{2k+1}{k+1} \zeta L_k(\zeta) - \frac{k}{k+1} \zeta L_{k-1}(\zeta), \quad k \geq 1 \quad (17)$$

In Table 1, this expression is used to calculate Legendre polynomials upto order 10.

Multivariate Legendre polynomials can be defined as products of univariate Legendre polynomials, similar to that of Hermite polynomials [44]. This can be constructed by considering products of different orders. We consider following sets of integers

$$\mathbf{i} = \{i_1, i_2, \dots, i_p\}, \quad i_k \geq 1 \quad (18)$$

$$\boldsymbol{\beta} = \{\beta_1, \beta_2, \dots, \beta_p\}, \quad \beta_k \geq 0 \quad (19)$$

The multivariate Legendre polynomial associated with sequence  $(\mathbf{i}, \boldsymbol{\beta})$  as the products of univariate Legendre polynomials

$$\mathcal{L}_{\mathbf{i}, \boldsymbol{\beta}}(\boldsymbol{\zeta}) = \prod_{k=1}^p L_{\beta_k}(\zeta_{i_k}) \quad (20)$$

The multivariate Legendre polynomials also satisfy the orthogonality condition with respect to the  $\mathcal{L}_2$  inner product norm in the respective dimension.

### 3.3. Projection in the basis of Legendre polynomials

We follow the idea of homogeneous chaos proposed by Wiener [29] involving Hermite polynomials. In the context of functions of random variables, Polynomial Chaos (PC) expansion [2] has been used extensively for uncertainty

Table 2  
Two-dimensional Legendre polynomial based homogeneous chaos basis up to 4th order.

$j$	$p$	Construction of $\Psi_j$	$\Psi_j$
0	$p = 0$	$L_0$	1
1	$p = 1$	$L_1(\zeta_1)$	$\zeta_1$
2		$L_1(\zeta_2)$	$\zeta_2$
3	$p = 2$	$L_2(\zeta_1)$	$3/2 \zeta_1^2 - 1/2$
4		$L_1(\zeta_1)L_1(\zeta_2)$	$\zeta_1 \zeta_2$
5		$L_2(\zeta_2)$	$3/2 \zeta_2^2 - 1/2$
6	$p = 3$	$L_3(\zeta_1)$	$5/2 \zeta_1^3 - 3/2 \zeta_1$
7		$L_2(\zeta_1)L_1(\zeta_2)$	$(3/2 \zeta_1^2 - 1/2)\zeta_2$
8		$L_1(\zeta_1)L_2(\zeta_2)$	$\zeta_1(3/2 \zeta_2^2 - 1/2)$
9		$L_3(\zeta_2)$	$5/2 \zeta_2^3 - 3/2 \zeta_2$
10	$p = 4$	$L_4(\zeta_1)$	$\frac{35}{8} \zeta_1^4 - \frac{15}{4} \zeta_1^2 + 3/8$
11		$L_3(\zeta_1)L_1(\zeta_2)$	$(5/2 \zeta_1^3 - 3/2 \zeta_1)\zeta_2$
12		$L_2(\zeta_1)L_2(\zeta_2)$	$(3/2 \zeta_1^2 - 1/2)(3/2 \zeta_2^2 - 1/2)$
13		$L_1(\zeta_1)L_3(\zeta_2)$	$\zeta_1(5/2 \zeta_2^3 - 3/2 \zeta_2)$
14		$L_4(\zeta_2)$	$\frac{35}{8} \zeta_2^4 - \frac{15}{4} \zeta_2^2 + 3/8$

propagation. When the basic random variables are Gaussian, multivariate Hermite polynomials can be used. The same idea can be extended to non-Gaussian random variables, provided more generalised functional basis are used [28]. It should be noted that the idea of homogeneous chaos cannot be directly applied to fuzzy variables as the polynomials are orthogonal over a given probability measure. However, mathematically the idea can still be used by considering a ‘unity’ within the inner product norm used for obtaining the orthogonality. We use multivariate Legendre polynomials considering the fact that the variables  $\zeta_i$  lie between  $[-1, 1]$  and they are independent for a given  $\alpha$ -cut. In a general setting, if a function  $f(\zeta)$  is a function of infinite number of variables  $\{\zeta_{i_k}\}$  and square integrable, it can be expanded in Homogeneous Chaos as

$$\begin{aligned}
 f(\zeta) &= \hat{y}_{i_0} h_0 + \sum_{i_1=1}^{\infty} \hat{y}_{i_1} \Gamma_1(\zeta_{i_1}) \\
 &+ \sum_{i_1=1}^{\infty} \sum_{i_2=1}^{i_1} \hat{y}_{i_1, i_2} \Gamma_2(\zeta_{i_1}, \zeta_{i_2}) + \sum_{i_1=1}^{\infty} \sum_{i_2=1}^{i_1} \sum_{i_3=1}^{i_2} \hat{y}_{i_1 i_2 i_3} \Gamma_3(\zeta_{i_1}, \zeta_{i_2}, \zeta_{i_3}) \\
 &+ \sum_{i_1=1}^{\infty} \sum_{i_2=1}^{i_1} \sum_{i_3=1}^{i_2} \sum_{i_4=1}^{i_3} \hat{y}_{i_1 i_2 i_3 i_4} \Gamma_4(\zeta_{i_1}, \zeta_{i_2}, \zeta_{i_3}, \zeta_{i_4}) + \dots
 \end{aligned}
 \tag{21}$$

Here  $\Gamma_p(\zeta_{i_1}, \zeta_{i_2}, \dots, \zeta_{i_m})$  is  $m$ -dimensional homogeneous chaos of order  $p$ . They can be obtained by products of one-dimensional Legendre polynomials. We refer to the book by Ghanem and Spanos [2] where similar procedure for Hermite polynomials is discussed. Truncating Eq. (21) up to finite number of terms, we can concisely write

$$f(\zeta) = \sum_{j=0}^{P-1} y_j \Psi_j(\zeta)
 \tag{22}$$

where the constant  $y_j$  and functions  $\Psi_j(\bullet)$  are effectively constants  $\hat{y}_k$  and functions  $\Gamma_k(\bullet)$  for corresponding indices. Eq. (22) can be viewed as the projection in the basis functions  $\Psi_j(\zeta)$  with corresponding ‘coordinates’  $y_j$ . The number of terms  $P$  in Eq. (22) depends on the number of variables  $m$  and maximum order of polynomials  $p$  as

$$P = \sum_{j=0}^p \frac{(m+j-1)!}{j!(m-1)!} = \binom{m+p}{p}
 \tag{23}$$

An example for two variables ( $m = 2$ ) with polynomial order 4 ( $p = 4$ ) is given in Table 2.

Table 3

Values of  $\langle \Psi_j(\xi), \Psi_j(\xi) \rangle$  for two variables ( $m = 2$ ) with polynomial order 4 ( $p = 4$ ).

$j$	0	1	2	3	4	5	6	7	8	9	10	11	12	13	14
$\langle \Psi_j(\xi), \Psi_j(\xi) \rangle$	1	1/3	1/3	1/5	1/9	1/5	1/7	1/15	1/15	1/7	1/9	1/21	1/25	1/21	1/9

A least-square error minimisation approach can be used to obtain the constants  $y_j$  in Eq. (22). We define the inner product norm in  $[-1, 1]^m$  as

$$\langle \bullet, \bullet \rangle = \frac{1}{V_m} \underbrace{\int_{-1}^1 \int_{-1}^1 \cdots \int_{-1}^1}_{m\text{-fold}} (\bullet)(\bullet) d\xi_1 d\xi_2 \cdots d\xi_m \quad (24)$$

Here the volume

$$V_m = 2^m \quad (25)$$

is used for normalisation so that for two constants  $a$  and  $b$  we have  $\langle a, b \rangle = ab$ . The error corresponding to Eq. (22) can be expressed as

$$\varepsilon = f(\xi) - \sum_{j=0}^{P-1} y_j \Psi_j(\xi) \quad (26)$$

Using the inner product norm in (24), the norm of the error can be obtained as

$$\chi^2 = \langle \varepsilon, \varepsilon \rangle \quad (27)$$

Differentiating this with respect to  $y_k$ , it can be shown that (Galerkin approach) the optimal values of  $y_k$  can be obtained by making the basis functions orthogonal to the error, that is,

$$\varepsilon \perp \Psi_k \quad \text{or} \quad \langle \Psi_k, \varepsilon \rangle = 0 \quad \forall k = 0, 2, \dots, P-1 \quad (28)$$

Substituting the expression of error from Eq. (26) into this equation we obtain

$$\sum_{j=0}^{P-1} y_j \langle \Psi_k(\xi), \Psi_j(\xi) \rangle = \langle \Psi_k(\xi), f(\xi) \rangle \quad (29)$$

Using the orthogonality property of the basis function we have  $\langle \Psi_k(\xi), \Psi_j(\xi) \rangle = c_k \delta_{jk}$ . Therefore, the constants  $y_k$  can be obtained as

$$y_k = \frac{\langle \Psi_k(\xi), f(\xi) \rangle}{\langle \Psi_k(\xi), \Psi_k(\xi) \rangle}, \quad \forall k = 0, 2, \dots, P-1 \quad (30)$$

The integration appearing in the numerator and denominator can be obtained using any standard procedure for multidimensional integrals. In particular, the denominator can be calculated explicitly. In Table 3 we show the values of  $\langle \Psi_j(\xi), \Psi_j(\xi) \rangle$  corresponding to  $\Psi_j(\xi)$  given in Table 2. Substituting the values of  $y_k$  from (30) into the expansion (22) we have

$$\hat{f}(\xi) = \sum_{j=0}^{P-1} \left[ \frac{\langle \Psi_j(\xi), f(\xi) \rangle}{\langle \Psi_j(\xi), \Psi_j(\xi) \rangle} \right] \Psi_j(\xi) \quad (31)$$

Here  $\hat{f}(\xi)$  is an approximation to the original function  $f(\xi)$  for polynomial order upto  $p$ . The accuracy of this approximation can improve indefinitely by considering higher-order polynomials. If the evaluation of the original function  $f(\xi)$  is expensive, the surrogate model  $\hat{f}(\xi)$  can be used instead of the original function. If  $\hat{f}(\xi)$  is a monotonic function, its bounds can be obtained by computing  $\hat{f}(\xi)$  only at the boundaries of the domain  $[-1, 1]^m$ . Therefore  $\hat{f}(\xi)$  needs to be evaluated  $2^m$  times in this case. This evaluation is computationally efficient as the polynomials  $\Psi_j(\xi)$



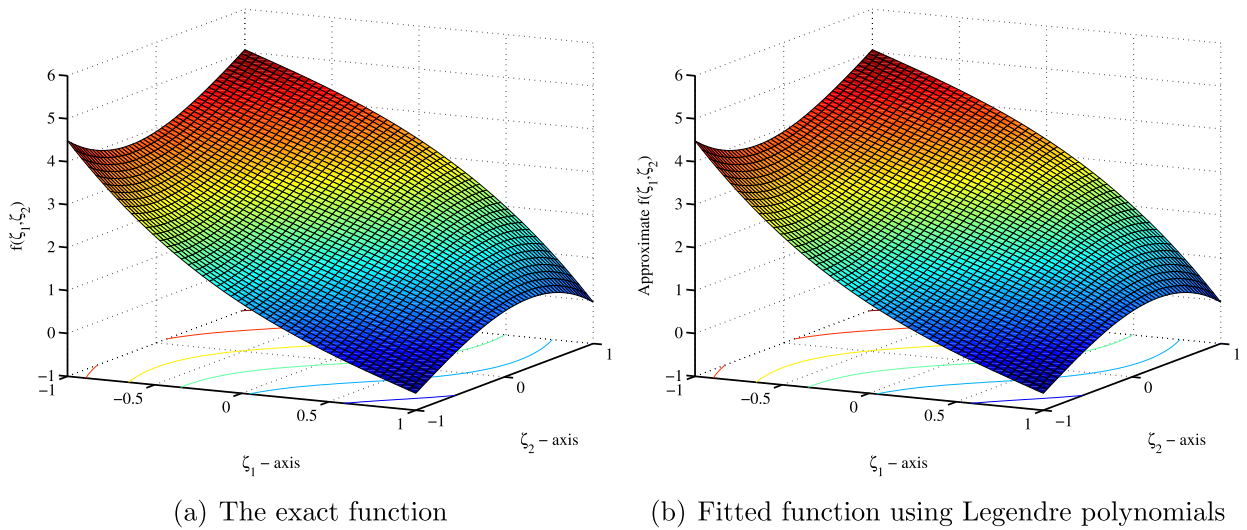


Fig. 2. The original function and the fitted function corresponding to Eq. (32).

are completely known in closed form. In the case of non-monotonic functions, the optimisation approach can be used to obtain the bounds of the functions. The main advantage is that the optimisation is carried out on a closed-form mathematical function that is efficient to compute with.

### 3.4. Example: Bounds of functions in two variables

To illustrate the application of the Galerkin projection approach, we consider two problems involving bounded variables. These bounds can be considered as bounds of a variable for a given  $\alpha$ -cut. For the first problem [45] we consider the function

$$\widehat{f}_1(\mathbf{x}) = \frac{89}{40} - \frac{\sqrt{2}}{1080}(x_1 + x_2 - 20)^3 + \frac{33}{140}(x_1 - x_2); \quad 4 \leq x_1, x_2 \leq 16 \tag{32}$$

As the first step, we transform the variables in  $[-1, 1]$  following (11). Omitting the notation  $\alpha$  for convenience, we have

$$x_1 = 6\xi_1 + 10 \quad \text{and} \quad x_2 = 6\xi_2 + 10 \tag{33}$$

Substituting these into Eq. (32) one obtains the function in the transformed variables as

$$f_1(\xi) = \frac{89}{40} - \frac{1}{5}\sqrt{2}(\xi_1 + \xi_2)^3 + \frac{99}{70}\xi_1 - \frac{99}{70}\xi_2 \tag{34}$$

Using Eq. (30), carrying out the 2-dimensional integration analytically, the values of  $y_j$  can be obtained as

$$\begin{aligned} y_1 &= \frac{89}{40}, & y_2 &= -\frac{8}{25}\sqrt{2} + \frac{99}{70} \\ y_3 &= -\frac{8}{25}\sqrt{2} - \frac{99}{70}, & y_7 &= -\frac{2}{25}\sqrt{2} \\ y_8 &= -2/5\sqrt{2}, & y_9 &= -2/5\sqrt{2} \quad \text{and} \quad y_{10} = \frac{2}{25}\sqrt{2} \end{aligned} \tag{35}$$

with all other values 0. In Fig. 2 the original function and the fitted function corresponding to Eq. (32) are shown. It can be seen that the approximation is very good. The maximum and the minimum values of the original function, appearing at the boundaries of the variables, are respectively 5.0536 and  $-0.6036$ . The exactly same values are obtained using the fitted function also. This demonstrates that the proposed approach using the Legendre polynomials can be used to propagate uncertainty for a given  $\alpha$ -cut.

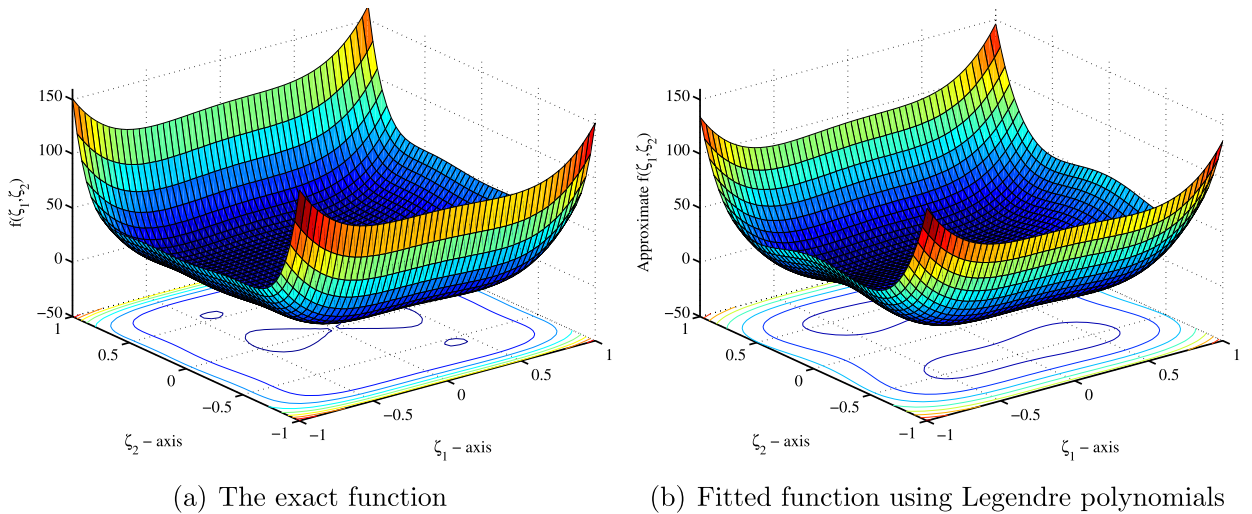


Fig. 3. The original function and the fitted function corresponding to Eq. (36).

The quality of the fitted function also depends on the nature of the non-linearity of the function to be approximated. We show an example when the proposed approach does not work very well for upto 4th-order polynomial approximation. For the second problem we consider the ‘Camelback’ function [46]

$$f_1(\mathbf{x}) = (4 - 2.1x_1^2 + x_1^4/3)x_1^2 + x_1x_2 + (-4 + 4x_2^2)x_2^2; \quad -3 \leq x_1 \leq 3; \quad -2 \leq x_2 \leq 2 \tag{36}$$

As before, we first transform the variables in  $[-1, 1]$  following (11). Omitting the notation  $\alpha$  for convenience, we have

$$x_1 = 3\xi_1 \quad \text{and} \quad x_2 = 2\xi_2 \tag{37}$$

Substituting these into Eq. (36) one obtains the function in the transformed variables as

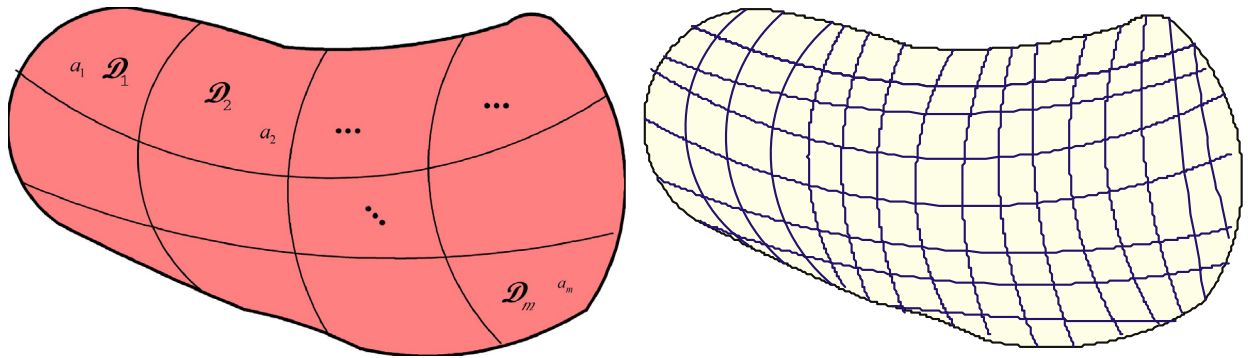
$$f_1(\boldsymbol{\xi}) = 9\left(4 - \frac{189}{10}\xi_1^2 + 27\xi_1^4\right)\xi_1^2 + 6\xi_1\xi_2 + 4(-4 + 16\xi_2^2)\xi_2^2 \tag{38}$$

Using Eq. (30), carrying out the 2-dimensional integration analytically, the values of  $y_j$  can be obtained as

$$\begin{aligned} y_1 &= \frac{21169}{1050}, & y_4 &= \frac{1488}{35}, & y_5 &= 6 \\ y_6 &= \frac{544}{21}, & y_{11} &= \frac{70956}{1925}, & y_{15} &= \frac{512}{35} \end{aligned} \tag{39}$$

with all other values 0. In Fig. 3 the original function and the fitted function corresponding to Eq. (36) are shown. The approximate function captures the general behaviour well. However, there are differences at the edge points in the domain where the extremum values occurs. The maximum and the minimum values of the original function, appearing at the boundaries of the variables, are respectively 162.9 and 150.9000. The corresponding values obtained using the 4th order polynomial approximation are 146.0688 and 134.0688, which implies errors of 10.3322% and 11.1539% respectively.

Any other polynomials can be used for approximating a function of fuzzy variables. However, it is only the Legendre polynomials which are orthogonal in the space of transformed variables. As a result, they guarantee the reconstruction of any smooth function within the space  $[-1, 1]^m$ . Next we extend this idea to boundary value problems involving fuzzy variables.



(a) Subdomains  $\mathcal{D}_i$  with Fuzzy parameter  $a_i$  for  $i = 1, 2, \dots, m$

(b) Finite element mesh

Fig. 4. Subdomains for the fuzzy parameter and finite element discretisation of the elliptic boundary value problem.

### 4. Fuzzy boundary value problems and finite element analysis

#### 4.1. Formulation of the problem

Boundary value problems are of primary interest for various engineering applications. We consider a bounded domain  $\mathcal{D} \in \mathbb{R}^d$  with piecewise Lipschitz boundary  $\partial\mathcal{D}$ , where  $d \leq 3$  is the spatial dimension. In this paper for simplicity we consider elliptic partial differential equations with Dirichlet boundary conditions given by

$$-\nabla[a(\mathbf{r})\nabla u(\mathbf{r})] = f(\mathbf{r}); \quad \mathbf{r} \text{ in } \mathcal{D}; \quad u(\mathbf{r}) = 0 \quad \text{on } \partial\mathcal{D} \tag{40}$$

Here  $a(\mathbf{r})$  is the fuzzy parameter and  $u(\mathbf{r})$  is fuzzy response quantity that we wish to calculate. In this section, the superscript  $\tilde{\bullet}$  is omitted for reasons of simplicity ( $\bullet$  is fuzzy variable). The parameter  $a(\mathbf{r})$  is a function of space  $\mathbf{r} \in \mathcal{D}$  and therefore contains infinite number of fuzzy variables considering the distributed nature of the problem. It is necessary to discretise  $a(\mathbf{r})$  for computational purposes. It is reasonable to assume that, for a complex system the parameter  $a(\mathbf{r})$  can take a finite number of different values depending on  $\mathbf{r}$ . We divide the domain  $\mathcal{D}$  into  $m$  non-overlapping subdomains as shown in Fig. 4(a). If we consider two subdomains  $\mathcal{D}_i, \mathcal{D}_k \in \mathcal{D}$ , then  $\mathcal{D}_i \cap \mathcal{D}_k = \emptyset$  and  $\mathcal{D} = \bigoplus_{i=1}^m \mathcal{D}_i$ . We define the discretised fuzzy variables  $a_i$  for all the subdomains as

$$a_i = a(\mathbf{r}); \quad \mathbf{r} \in \mathcal{D}_i, \quad \forall i = 1, 2, \dots, m \tag{41}$$

In this way we effectively discretised  $a(\mathbf{r})$  in to a finite number of fuzzy variables. Symbolically we can write

$$a = \bigoplus_{i=1}^m a_i \tag{42}$$

where  $\bigoplus$  denotes the sum taking the subdomains in Eq. (41) into account. In Fig. 4(b) the finite element (FE) mesh corresponding to the problem is shown. The finite element (FE) mesh in general will be different from the discretisation of the fuzzy parameter  $a(\mathbf{r})$ . Normally a particular subdomain  $\mathcal{D}_i$  is expected to contain several finite elements, which implies that the finite element discretisation is expected to be finer compared to the discretisation of the fuzzy parameter. This is due to the fact that the spatial variability of the response quantity is in general expected to be greater than the variability of system parameters. The element stiffness matrix can be obtained following the conventional finite element approach [1] as

$$\mathbf{K}_e = \int_{\mathcal{D}_e} a(\mathbf{r})\mathbf{B}^{(e)T}(\mathbf{r})\mathbf{B}^{(e)}(\mathbf{r}) d\mathbf{r} = a_i \int_{\mathcal{D}_e} \mathbf{B}^{(e)T}(\mathbf{r})\mathbf{B}^{(e)}(\mathbf{r}) d\mathbf{r}; \quad \mathbf{r} \in \mathcal{D}_i \tag{43}$$

The second equality arises due to the fact that each element is contained in a single subdomain  $\mathcal{D}_i$ , that is, none of the elements overlaps into another subdomain. In the above equations  $\mathbf{B}^{(e)}(\mathbf{r})$  is a deterministic matrix related to the

shape function used to interpolate the solution within the element  $e$ . For elliptic type problems it can be shown [1] that  $\mathbf{B}^{(e)}(\mathbf{r}) = \nabla \mathbf{N}^{(e)}(\mathbf{r})$ . Suppose  $\underline{a}_i^{(\alpha)}$  and  $\bar{a}_i^{(\alpha)}$  denotes the lower and upper bound of the fuzzy variable  $\tilde{a}_i$  for a given  $\alpha$ -cut. We transform  $\tilde{a}_i$  into the standard variable  $\zeta_i \in [-1, 1]$  for every  $\alpha$ -cut following Eq. (11) as

$$a_i^{(\alpha)} = \left( \frac{\bar{a}_i^{(\alpha)} - \underline{a}_i^{(\alpha)}}{2} \right) \zeta_i + \frac{(\bar{a}_i^{(\alpha)} + \underline{a}_i^{(\alpha)})}{2} \tag{44}$$

Substituting this into Eq. (43) we have

$$\mathbf{K}_e^{(\alpha)} = \mathbf{K}_{e_0}^{(\alpha)} + \zeta_i \mathbf{K}_{e_i}^{(\alpha)} \tag{45}$$

where the crisp and fuzzy parts of the element stiffness matrix is given by

$$\mathbf{K}_{e_0}^{(\alpha)} = \frac{(\bar{a}_i^{(\alpha)} + \underline{a}_i^{(\alpha)})}{2} \int_{\mathcal{D}_e} \mathbf{B}^{(e)T}(\mathbf{r}) \mathbf{B}^{(e)}(\mathbf{r}) d\mathbf{r} \tag{46}$$

and

$$\mathbf{K}_{e_i}^{(\alpha)} = \frac{(\bar{a}_i^{(\alpha)} - \underline{a}_i^{(\alpha)})}{2} \int_{\mathcal{D}_e} \mathbf{B}^{(e)T}(\mathbf{r}) \mathbf{B}^{(e)}(\mathbf{r}) d\mathbf{r}; \quad \mathbf{r} \in \mathcal{D}_i \tag{47}$$

The global stiffness matrix can be obtained by the usual finite element assembly procedure [1] and taking account of the domains of the discretised fuzzy variables. The finite element equation for a given  $\alpha$ -cut can be expressed as

$$\mathbf{K}^{(\alpha)} \mathbf{u}^{(\alpha)} = \mathbf{f} \tag{48}$$

In the preceding equation  $\mathbf{f} \in \mathbb{R}^n$  is the global forcing vector and the global stiffness matrix  $\mathbf{K}^{(\alpha)} \in \mathbb{R}^{n \times n}$  can be expressed as

$$\mathbf{K}^{(\alpha)} = \mathbf{K}_0^{(\alpha)} + \sum_{i=1}^M \zeta_i \mathbf{K}_i^{(\alpha)} \tag{49}$$

Here  $n$  is the degrees of freedom of the system and it depends on the number of finite element used for the discretisation. In the above equation, the crisp part of the global stiffness matrix

$$\mathbf{K}_0^{(\alpha)} = \bigoplus_e \mathbf{K}_{e_0}^{(\alpha)} \tag{50}$$

where  $\bigoplus_e$  denotes the summation over all the elements. The fuzzy parts of the stiffness matrix related to the variable  $\zeta_j$  can be given by

$$\mathbf{K}_i^{(\alpha)} = \bigoplus_{e: \mathbf{r} \in \mathcal{D}_i} \mathbf{K}_{e_i}^{(\alpha)} \tag{51}$$

where  $\bigoplus_{e: \mathbf{r} \in \mathcal{D}_i}$  denotes the summation over those elements for which the domain belongs to  $\mathcal{D}_i$ . The parts of the matrix  $\mathbf{K}_i^{(\alpha)}$  will contain zeros for which  $\mathbf{r} \notin \mathcal{D}_i$ . An expression of the stiffness matrix similar to Eq. (49) can alternatively obtained directly for complex systems where different subsystems may contain different fuzzy variables. In that case  $\mathbf{K}_i^{(\alpha)}$  would be block matrices, influenced by only the transformed fuzzy variable  $\zeta_i$  within a particular subsystem. From Eq. (47) observe that the norm of the coefficient matrices  $\mathbf{K}_i^{(\alpha)}$  in Eq. (49) is proportional to the difference between the upper and lower values of the interval. This implies that the norm of these matrices would be larger for larger variability. Next we obtain a fuzzy description of the response  $\mathbf{u}$  based on the orthogonal polynomial approach where it can be seen that the coefficient matrices  $\mathbf{K}_i^{(\alpha)}$  play a key role.

### 4.2. Galerkin approach

In Section 3.3 it was shown the a scalar function of fuzzy variables can be projected in the basis of Legendre polynomials. Here this idea is extended to vector functions. The elements of the solution vector  $\mathbf{u}^{(\alpha)}$  in the fuzzy finite element equation (48) can be viewed as nonlinear functions of the variables  $\zeta_j \in [-1, 1]$ . Similar to Eq. (22), we project the solution vector  $\mathbf{u}(\zeta) \in \mathbb{R}^n$  in the basis of Legendre polynomials as

$$\mathbf{u}^{(\alpha)}(\zeta) = \sum_{j=0}^{P-1} \mathbf{u}_j^{(\alpha)} \Psi_j(\zeta) \tag{52}$$

We aim to obtain the coefficient vectors  $\mathbf{u}_j \in \mathbb{R}^n$  using a Galerkin type of error minimisation approach.

Substituting expansion of  $\mathbf{u}^{(\alpha)}(\zeta)$  in the governing equation (48), the error vector can be obtained as

$$\boldsymbol{\varepsilon}^{(\alpha)} = \left( \sum_{i=0}^M \mathbf{K}_i^{(\alpha)} \zeta_i \right) \left( \sum_{j=1}^{P-1} \mathbf{u}_j^{(\alpha)} \Psi_j(\zeta) \right) - \mathbf{f} \in \mathbb{R}^n \tag{53}$$

where  $\zeta_0 = 1$  is used to simplify the first summation expression. The expression (52) is viewed as a projection where  $\Psi_j(\zeta)$  are the orthogonal basis functions and  $\mathbf{u}_j^{(\alpha)}$  are the unknown ‘coordinates’ to be determined. We wish to obtain the vectors  $\mathbf{u}_j^{(\alpha)}$  using the Galerkin approach so that the error is made orthogonal to the basis functions, that is, mathematically

$$\boldsymbol{\varepsilon}^{(\alpha)} \perp \Psi_k(\zeta) \quad \text{or} \quad \langle \Psi_k(\zeta), \boldsymbol{\varepsilon}^{(\alpha)} \rangle = 0, \quad \forall k = 0, 2, \dots, P - 1 \tag{54}$$

Imposing this condition and using the expression of  $\boldsymbol{\varepsilon}^{(\alpha)}$  from Eq. (53) one has

$$\left\langle \Psi_k(\zeta), \left( \sum_{i=0}^M \mathbf{K}_i^{(\alpha)} \zeta_i \right) \left( \sum_{j=1}^{P-1} \mathbf{u}_j^{(\alpha)} \Psi_j(\zeta) \right) - \mathbf{f} \right\rangle = 0, \quad \forall k = 0, 2, \dots, P - 1 \tag{55}$$

Interchanging the summation operations, this can be simplified to

$$\sum_{j=1}^{P-1} \sum_{i=0}^M \mathbf{K}_i^{(\alpha)} \langle \zeta_i \Psi_j(\zeta) \Psi_k(\zeta) \rangle \mathbf{u}_j^{(\alpha)} - \langle \Psi_k(\zeta) \mathbf{f} \rangle = 0, \quad \forall k = 0, 2, \dots, P - 1 \tag{56}$$

Introducing the notations

$$c_{ijk} = \langle \zeta_i \Psi_j(\zeta) \Psi_k(\zeta) \rangle \in \mathbb{R} \quad \text{and} \tag{57}$$

$$\mathbf{f}_k = \langle \Psi_k(\zeta) \mathbf{f} \rangle \in \mathbb{R}^n \tag{58}$$

one can express Eq. (56) as

$$\sum_{j=1}^{P-1} \sum_{i=0}^M c_{ijk} \mathbf{K}_i^{(\alpha)} \mathbf{u}_j^{(\alpha)} = \mathbf{f}_k, \quad \forall k = 0, 2, \dots, P - 1 \tag{59}$$

In this paper the forcing is assumed to be deterministic. Therefore,  $\mathbf{f}_k = \langle \Psi_k(\zeta) \mathbf{f} \rangle = \langle \Psi_k(\zeta) \rangle \mathbf{f}$ . Using the definition of the orthogonal functions it can be easily shown that  $\langle \Psi_1(\zeta) \rangle = 1$  and  $\langle \Psi_k(\zeta) \rangle = 0$  for any other values of  $k$ . The constants  $c_{ijk}$  can be obtained in closed-form by performing the necessary integrals. It turns out that many of the  $c_{ijk}$  becomes 0. As an example, for the case two variables with fourth-order homogeneous chaos, the nonzero values of the constants  $c_{ijk}$  are shown in Table 4. Once the values of  $c_{ijk}$  and  $\mathbf{f}_k$  are obtained, further defining

$$\mathbf{K}_{jk}^{(\alpha)} = \sum_{i=0}^M c_{ijk} \mathbf{K}_i^{(\alpha)} \in \mathbb{R}^{n \times n} \tag{60}$$

one can rewrite Eq. (59) as

Table 4  
 Values of  $c_{1jk}$  and  $c_{2jk}$  defined in Eq. (57) for two dimensional Legendre polynomial based homogeneous chaos basis up to 4th order.

$j$	$k$	$c_{1jk}$	$j$	$k$	$c_{2jk}$
0	1	1/3	0	2	1/3
1	0	1/3	1	4	1/9
1	3	2/15	2	0	1/3
2	4	1/9	2	5	2/15
3	1	2/15	3	7	1/15
3	6	3/35	4	1	1/9
4	2	1/9	4	8	2/45
4	7	2/45	5	2	2/15
5	8	1/15	5	9	3/35
6	3	3/35	6	11	1/21
6	10	4/63	7	3	1/15
7	4	2/45	7	12	2/75
7	11	1/35	8	4	2/45
8	5	1/15	8	13	1/35
8	12	2/75	9	5	3/35
9	13	1/21	9	14	4/63
10	6	4/63	11	6	1/21
11	7	1/35	12	7	2/75
12	8	2/75	13	8	1/35
13	9	1/21	14	9	4/63

$$\sum_{j=1}^{P-1} \mathbf{K}_{jk}^{(\alpha)} \mathbf{u}_j = \mathbf{f}_k, \quad \forall k = 0, 2, \dots, P - 1 \tag{61}$$

For all values of  $k$ , this equation can be expressed in a matrix form as

$$\begin{bmatrix} \mathbf{K}_{0,0}^{(\alpha)} & \mathbf{K}_{0,1}^{(\alpha)} & \cdots & \mathbf{K}_{0,P-1}^{(\alpha)} \\ \mathbf{K}_{1,0}^{(\alpha)} & \mathbf{K}_{1,1}^{(\alpha)} & \cdots & \mathbf{K}_{1,P-1}^{(\alpha)} \\ \vdots & \vdots & \ddots & \vdots \\ \mathbf{K}_{P-1,0}^{(\alpha)} & \mathbf{K}_{P-1,1}^{(\alpha)} & \cdots & \mathbf{K}_{P-1,P-1}^{(\alpha)} \end{bmatrix} \begin{Bmatrix} \mathbf{u}_0^{(\alpha)} \\ \mathbf{u}_1^{(\alpha)} \\ \vdots \\ \mathbf{u}_{P-1}^{(\alpha)} \end{Bmatrix} = \begin{Bmatrix} \mathbf{f}_0 \\ \mathbf{f}_1 \\ \vdots \\ \mathbf{f}_{P-1} \end{Bmatrix} \tag{62}$$

or in a compact notation

$$\mathcal{K}^{(\alpha)} \mathbf{U}^{(\alpha)} = \mathcal{F} \tag{63}$$

where  $\mathcal{K}^{(\alpha)} \in \mathbb{R}^{nP \times nP}$ ,  $\mathbf{U}^{(\alpha)}, \mathcal{F} \in \mathbb{R}^{nP}$ . This equation needs to be solved for every  $\alpha$ -cut. Once all  $\mathbf{u}_j^{(\alpha)}$  for  $j = 0, 2, \dots, P - 1$  are obtained, the solution vector can be obtained from (52) for every  $\alpha$ -cut. The fuzzy description of the vector  $\mathbf{u}$  can be obtained by obtaining minimum and maximum values of  $\mathbf{u}^{(\alpha)}$  for all  $\alpha$ -cuts. In this way the complete fuzzy description of the solution can be obtained by using the proposed orthogonal function approach.

### 4.3. Model reduction

The main computational challenge posed by the method proposed here is the solution of the set of linear equations in (62), which of size  $nP$ . The value of the number of terms  $P$  depends on the number of fuzzy variables  $M$  and the order of the chaos expansion  $r$  as given by Eq. (23). In Table 5 some values of  $P$  are shown for different numbers of fuzzy variables and order of chaos expansions. It can be seen that  $P$  increases significantly with  $M$  and  $r$ . The value of  $n$  depends on the finite element discretisation and can be large for complex problems. Therefore for practical problems  $nP$  can be very large. For large systems with many fuzzy variables, the solution of Eq. (62) can be a formidable task as one needs to solve Eq. (62) for every  $\alpha$ -cut. The computational complexity of the matrix inversion problem scales in cubically with the dimension of the matrix in the worse case [47]. Therefore, the computational time for solving Eq. (62) is in  $\mathcal{O}(P^3 n^3)$ . Since  $P$  is fixed by Eq. (23), we aim to reduce the dimension of the system using an eigensolution decomposition.

Table 5  
Values of the number of terms  $P$  for different number of fuzzy variables ( $M$ ) and order of chaos expansion  $r$ .

$M$	2	3	5	10	20	50	100
1st order ( $r = 1$ )	3	4	6	11	21	51	101
2nd order ( $r = 2$ )	6	10	21	66	231	1326	5151
3rd order ( $r = 3$ )	10	20	56	286	1771	23426	176851
4th order ( $r = 4$ )	15	35	126	1001	10626	316251	4598126

To illustrate the motivation behind the proposed reduced method, first consider the deterministic system for a given  $\alpha$ -cut

$$\mathbf{K}_0^{(\alpha)} \mathbf{u}_0^{(\alpha)} = \mathbf{f} \tag{64}$$

For most finite element applications,  $\mathbf{K}_0^{(\alpha)}$  is a symmetric and positive definite matrix. Its eigenvalues are positive and its eigenvectors form a complete orthonormal basis. The eigenvalue problem can be expressed as

$$\mathbf{K}_0^{(\alpha)} \boldsymbol{\phi}_k^{(\alpha)} = \lambda_{0_k}^{(\alpha)} \boldsymbol{\phi}_k^{(\alpha)}; \quad k = 1, 2, \dots, n \tag{65}$$

For notational convenience, define the matrix of eigenvalues and eigenvectors

$$\Lambda_0^{(\alpha)} = \text{diag}[\lambda_{0_1}^{(\alpha)}, \lambda_{0_2}^{(\alpha)}, \dots, \lambda_{0_n}^{(\alpha)}] \in \mathbb{R}^{n \times n} \quad \text{and} \quad \boldsymbol{\Phi}^{(\alpha)} = [\boldsymbol{\phi}_1^{(\alpha)}, \boldsymbol{\phi}_2^{(\alpha)}, \dots, \boldsymbol{\phi}_n^{(\alpha)}] \in \mathbb{R}^{n \times n} \tag{66}$$

Eigenvalues are ordered in the ascending order so that  $\lambda_{0_1}^{(\alpha)} < \lambda_{0_2}^{(\alpha)} < \dots < \lambda_{0_n}^{(\alpha)}$ . Since  $\boldsymbol{\Phi}^{(\alpha)}$  is an orthogonal matrix we have  $\boldsymbol{\Phi}^{(\alpha)-1} = \boldsymbol{\Phi}^{(\alpha)T}$  so that the following identities can be easily established

$$\boldsymbol{\Phi}^{(\alpha)T} \mathbf{K}_0^{(\alpha)} \boldsymbol{\Phi}^{(\alpha)} = \Lambda_0^{(\alpha)}, \quad \mathbf{K}_0^{(\alpha)} = \boldsymbol{\Phi}^{-T} \Lambda_0^{(\alpha)} \boldsymbol{\Phi}^{(\alpha)-1} \quad \text{and} \quad \mathbf{K}_0^{(\alpha)-1} = \boldsymbol{\Phi}^{(\alpha)} \Lambda_0^{(\alpha)-1} \boldsymbol{\Phi}^{(\alpha)T} \tag{67}$$

Using these, the solution of Eq. (64) can be expressed as

$$\mathbf{u}_0^{(\alpha)} = \mathbf{K}_0^{(\alpha)-1} \mathbf{f} = \boldsymbol{\Phi}^{(\alpha)} \Lambda_0^{(\alpha)-1} (\boldsymbol{\Phi}^{(\alpha)T} \mathbf{f}) = \sum_{k=1}^n \frac{\boldsymbol{\phi}_k^{(\alpha)T} \mathbf{f}}{\lambda_{0_k}^{(\alpha)}} \boldsymbol{\phi}_k^{(\alpha)} \tag{68}$$

The series (68) can be truncated based on the magnitude of the eigenvalues as the higher terms becomes smaller. Therefore one could only retain the dominant terms in the series. A similar model reduction technique has been widely used within the proper orthogonal decomposition method [48] where the eigenvalues of a symmetric positive definite matrix are used. One can select a small value  $\epsilon$  such that  $\lambda_{0_1}^{(\alpha)} / \lambda_{0_p}^{(\alpha)} < \epsilon$  for some value of  $p$ . Therefore, truncating the series in (68) one can have

$$\mathbf{u}_0^{(\alpha)} \approx \sum_{j=1}^p \frac{\boldsymbol{\phi}_j^{(\alpha)T} \mathbf{f}}{\lambda_{0_j}^{(\alpha)}} \boldsymbol{\phi}_j^{(\alpha)} \tag{69}$$

We use this simple idea to develop the model reduction approach.

We form the reduced matrix of dominant eigenvalues and eigenvectors as

$$\Lambda_{0_p}^{(\alpha)} = \text{diag}[\lambda_{0_1}^{(\alpha)}, \lambda_{0_2}^{(\alpha)}, \dots, \lambda_{0_p}^{(\alpha)}] \in \mathbb{R}^{p \times p} \quad \text{and} \quad \boldsymbol{\Phi}_p^{(\alpha)} = [\boldsymbol{\phi}_1^{(\alpha)}, \boldsymbol{\phi}_2^{(\alpha)}, \dots, \boldsymbol{\phi}_p^{(\alpha)}] \in \mathbb{R}^{n \times p} \tag{70}$$

Let us introduce the transformation

$$\mathbf{u}(\boldsymbol{\zeta}) = \boldsymbol{\Phi}_p^{(\alpha)} \mathbf{y}(\boldsymbol{\zeta}) \tag{71}$$

where  $\mathbf{y} \in \mathbb{R}^p$  is the new unknown fuzzy vector to be determined. Substituting in the original equation (48) and premultiplying by  $\boldsymbol{\Phi}_p^{(\alpha)T}$  we have

$$\left[ \Lambda_{0_p}^{(\alpha)} + \sum_{i=1}^M \zeta_i \tilde{\mathbf{K}}_i^{(\alpha)} \right] \mathbf{y}(\boldsymbol{\zeta}) = \tilde{\mathbf{f}} \tag{72}$$

where the transformed reduced matrices and vector are given by

$$\tilde{\mathbf{K}}_i^{(\alpha)} = \Phi_p^{(\alpha)T} \mathbf{K}_i^{(\alpha)} \Phi_p^{(\alpha)} \in \mathbb{R}^{P \times P}; \quad i = 1, 2, \dots, M \quad \text{and} \quad \tilde{\mathbf{f}} = \Phi_p^{(\alpha)T} \mathbf{f} \tag{73}$$

The main idea is to expand the reduced fuzzy vector  $\mathbf{y}(\boldsymbol{\zeta})$  with a Legendre Polynomial Chaos expansion. For a selected order, the polynomial  $\Psi_k(\boldsymbol{\zeta})$  will be identical to the ones used for the system with all the degrees of. Therefore, we have

$$\mathbf{y}^{(\alpha)}(\boldsymbol{\zeta}) = \sum_{j=0}^{P-1} \mathbf{y}_j^{(\alpha)} \Psi_j(\boldsymbol{\zeta}) \tag{74}$$

The unknown vectors  $\mathbf{y}_j^{(\alpha)}$  can be obtained by substituting  $\mathbf{y}^{(\alpha)}(\boldsymbol{\zeta})$  from the above expressions into the reduced (72) and minimising the error using the standard Galerkin approach [2]. It can be shown that we need to solve a  $pP \times pP$  system of linear equation to obtain all  $\mathbf{y}_j^{(\alpha)} \in \mathbb{R}^P$ :

$$\begin{bmatrix} \tilde{\mathbf{K}}_{0,0}^{(\alpha)} & \tilde{\mathbf{K}}_{0,1}^{(\alpha)} & \cdots & \tilde{\mathbf{K}}_{0,P-1}^{(\alpha)} \\ \tilde{\mathbf{K}}_{1,0}^{(\alpha)} & \tilde{\mathbf{K}}_{1,1}^{(\alpha)} & \cdots & \tilde{\mathbf{K}}_{1,P-1}^{(\alpha)} \\ \vdots & \vdots & \ddots & \vdots \\ \tilde{\mathbf{K}}_{P-1,0}^{(\alpha)} & \tilde{\mathbf{K}}_{P-1,1}^{(\alpha)} & \cdots & \tilde{\mathbf{K}}_{P-1,P-1}^{(\alpha)} \end{bmatrix} \begin{Bmatrix} \mathbf{y}_0^{(\alpha)} \\ \mathbf{y}_1^{(\alpha)} \\ \vdots \\ \mathbf{y}_{P-1}^{(\alpha)} \end{Bmatrix} = \begin{Bmatrix} \tilde{\mathbf{f}}_0 \\ \tilde{\mathbf{f}}_1 \\ \vdots \\ \tilde{\mathbf{f}}_{P-1} \end{Bmatrix} \tag{75}$$

Once  $\mathbf{y}_j^{(\alpha)}$  are obtained by solving Eq. (75), they can be substituted in the polynomial expansion (74) to obtain the response in the reduced coordinate  $\mathbf{y}^{(\alpha)}(\boldsymbol{\zeta})$ . The response in the original coordinate can be obtained by the transformation (71). For many practical problems  $p \ll n$ . Since the computational complexity of the matrix inversion problem scales in cubically with the dimension of the matrix,  $\mathcal{O}(P^3 p^3) \ll \mathcal{O}(P^3 n^3)$ . As a result the reduced approach for every  $\alpha$ -cut can offer significant overall computational reduction. This is discussed further in the numerical examples later in the next section.

### 5. Numerical examples

#### 5.1. Problem description

To illustrate the proposed method, we consider the axial deformation of a rod subjected to a constant pulling force [32]. The equilibrium equation can be expressed by

$$-\frac{\partial}{\partial x} \left\{ EA(x) \frac{\partial u(x)}{\partial x} \right\} = f(x) \tag{76}$$

where  $u(x)$  is the axial deformation and  $EA(x)$  is the axial rigidity of the rod. We consider the axial rigidity as a fuzzy parameter. It is assumed that the value of  $EA(x)$  is constant with respect to  $x$  between two non-overlapping subdomains, defined as

$$\mathcal{D}_1 \equiv [0, L_1] \quad \text{and} \quad \mathcal{D}_2 \equiv [L_1, L_2] \tag{77}$$

The total length of the rod is  $L = L_1 + L_2$ . We therefore define two fuzzy variables depending on the value of  $x$  as

$$EA(x) = EA_1, \quad x \in \mathcal{D}_1 \tag{78}$$

$$EA(x) = EA_2, \quad x \in \mathcal{D}_2 \tag{79}$$

It is considered that the rod is fixed at one end as is being pulled at the other end. The system to be studied is shown in Fig. 5. The total length of the rod is assumed to be  $L = 2$  m. The length of the two subdomains are respectively  $L_1 = 1$  m and  $L_2 = 1$  m. The crisp values of the axial rigidities of the two sections are  $\overline{EA}_1 = 20 \times 10^7$  N,  $\overline{EA}_2 = 5 \times 10^7$  N. The applied forcing is assumed to be  $F = 1$  kN. For the numerical calculations, each section is divided into 50 finite elements. The total degrees of freedom of the system, that is the dimension  $n = 100$ . We are interested in the fuzzy description of the deformation of the rod  $u(x)$ . In the following sections two cases are considered, namely (a) when the membership functions are linear (that is, the intervals in the fuzzy variable change linearly with  $\alpha$ ), and (b) when the membership functions are nonlinear (that is, the intervals in the fuzzy variable change nonlinearly with  $\alpha$ ). Further, the reduced computational approach proposed before is also illustrated numerically.



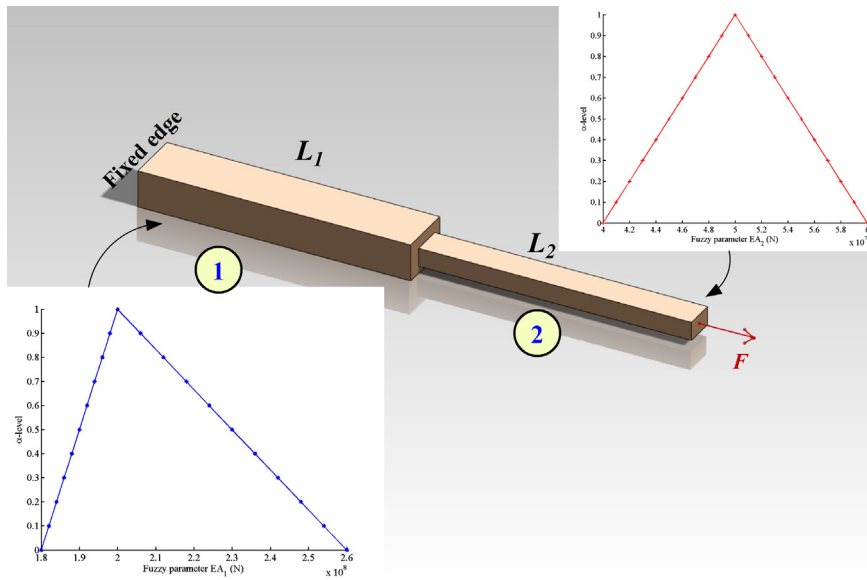


Fig. 5. A cantilever rod subjected to an axial force modelled using two fuzzy variables. Numerical values for the problem are selected as:  $L_1 = 1$  m,  $L_2 = 1$  m, crisp values  $\overline{EA}_1 = 20 \times 10^7$  N,  $\overline{EA}_2 = 5 \times 10^7$  N,  $F = 1$  kN. The linear (triangular) membership functions for the two variables are shown in the figure.

### 5.2. Fuzzy variables with linear membership functions

We consider the simplest case when the two fuzzy variables  $EA_1$  and  $EA_2$  have linear membership functions. For this case the intervals of the fuzzy variables vary linearly with  $\alpha$ . The variation is shown in Fig. 5. At  $\alpha = 0$  we have the maximum variability

$$18 \times 10^7 \leq EA_1 \leq 26 \times 10^7 \quad \text{and} \quad 4 \times 10^7 \leq EA_2 \leq 6 \times 10^7 \tag{80}$$

This implies a variability between  $-10\%$  and  $30\%$  for  $EA_1$  and  $\pm 20\%$  for  $EA_2$ . The maximum and minimum values of the interval for a given  $\alpha$ -cut can be described for the two fuzzy variables as

$$EA_{1_{\min}} = \overline{EA}_1(0.9 + 0.1\alpha) \quad \text{and} \quad EA_{1_{\max}} = \overline{EA}_1(1.3 - 0.3\alpha) \tag{81}$$

$$EA_{2_{\min}} = \overline{EA}_2(0.8 + 0.2\alpha) \quad \text{and} \quad EA_{2_{\max}} = \overline{EA}_2(1.2 - 0.2\alpha) \tag{82}$$

The membership functions for both fuzzy variables are triangular in nature, with  $EA_1$  is nonsymmetric while  $EA_2$  is symmetric. Substituting the value of  $EA(x)$  into Eq. (76) and discretising using the finite element method we have

$$\mathbf{K} = \mathbf{K}_0 + \zeta_1 \mathbf{K}_1^{(\alpha)} + \zeta_2 \mathbf{K}_2^{(\alpha)} \tag{83}$$

Here  $\mathbf{K}_0 \in \mathbb{R}^{100 \times 100}$  is the stiffness matrix corresponding to the crisp values,  $\mathbf{K}_1^{(\alpha)}$  and  $\mathbf{K}_2^{(\alpha)}$  are the coefficient matrices corresponding to a given  $\alpha$ -cut. The matrices  $\mathbf{K}_1^{(\alpha)}$  and  $\mathbf{K}_2^{(\alpha)}$  are block matrices corresponding to length  $L_1$  and  $L_2$  as shown in Fig. 5.

We consider the fuzzy description of the displacement response of the rod at two points, namely at the mid point (where the section area changes) and at the end point. For the numerical calculations, 11 values, uniformly spaced at different  $\alpha$ -cuts ( $0, 0.1, 0.2, \dots, 1.0$ ) are selected. Results obtained from the proposed Legendre polynomial based approach are compared to the direct simulation results in Fig. 6. We solve Eq. (62) to obtain  $\mathbf{u}_j^{(\alpha)}$  for all the 10 values of  $\alpha$ -cuts ( $\alpha = 0$  is the crisp case for which the polynomial expansion is not necessary). For the first-, second- and fourth-order polynomial approximations with two variables, 3, 6 and 15 terms are necessary (see Table 5). This in turn results in the dimension of Eq. (62) as 300, 600 and 1500 respectively. For the direct simulation approach, Eq. (48) is solved for different 5000 values of  $\zeta_1$  and  $\zeta_2$  and maximum and minimum values are taken from all the output values for each  $\alpha$ -cuts. It can be seen that except the first-order approach, the proposed orthogonal polynomial

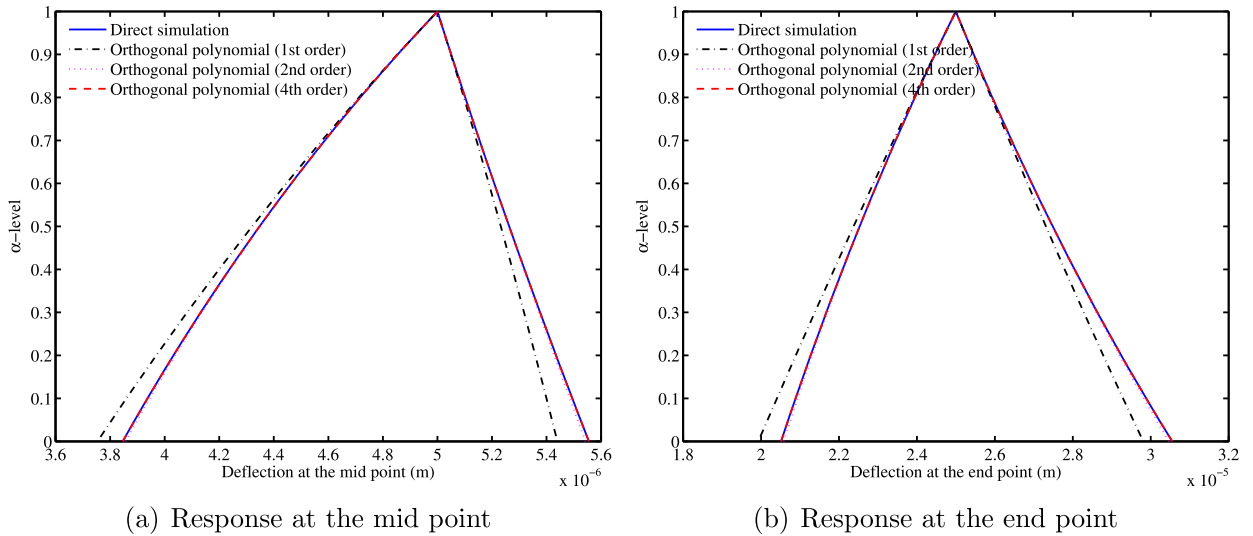


Fig. 6. Fuzzy description of the response of the rod at two points computed using different order of Legendre polynomial based homogeneous chaos and direct simulation.

Table 6

Percentage error in the displacement at the mid point of the rod computed using different order of Legendre polynomial based homogeneous chaos.

$\alpha$ -cut	1st order		2nd order		4th order	
	min	max	min	max	min	max
0.0	2.4136	2.0837	0.2669	0.2280	0.0026	0.0026
0.1	1.9713	1.7254	0.1976	0.1713	0.0016	0.0016
0.2	1.5711	1.3944	0.1410	0.1241	0.0009	0.0009
0.3	1.2138	1.0925	0.0961	0.0858	0.0005	0.0005
0.4	0.9001	0.8219	0.0615	0.0558	0.0002	0.0002
0.5	0.6312	0.5848	0.0362	0.0334	0.0001	0.0001
0.6	0.4081	0.3837	0.0189	0.0177	0.0000	0.0000
0.7	0.2320	0.2214	0.0081	0.0077	0.0000	0.0000
0.8	0.1042	0.1010	0.0025	0.0024	0.0000	0.0000
0.9	0.0264	0.0259	0.0003	0.0003	0.0000	0.0000
1.0	0.0000	0.0000	0.0000	0.0000	0.0000	0.0000

method matched with the direct simulation results very well. The percentage errors corresponding to the responses at the two points shown in Fig. 6, are given in Table 6 and Table 7 respectively. The percentage errors are calculated by considering the direct simulation results as the benchmarks. One can observe that the error is zero up to 4th decimal place for higher values of  $\alpha$ -cut. For very low values of  $\alpha$ -cut and with the first-order approximation, some errors can be observed. Therefore, we conclude that a second or higher order approximation is reasonable for this problem.

### 5.3. Fuzzy variables with nonlinear membership functions

Now we consider the case when the two fuzzy variables  $EA_1$  and  $EA_2$  have nonlinear membership functions. Therefore, the intervals of both the fuzzy variables vary nonlinearly with  $\alpha$ . The variation is shown in Fig. 7. These nonlinear membership functions are selected for illustrative purposes only. One can choose any other membership functions as the method proposed is independent of this choice. At  $\alpha = 0$  we have the maximum variability

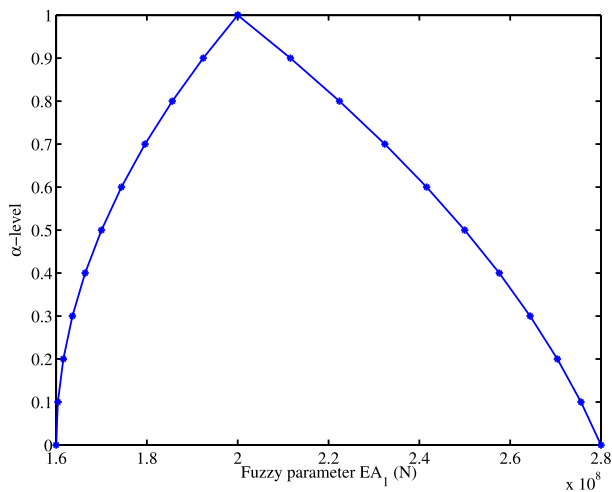
$$16 \times 10^7 \leq EA_1 \leq 28 \times 10^7 \quad \text{and} \quad 3.5 \times 10^7 \leq EA_2 \leq 7 \times 10^7 \tag{84}$$

This implies a variability between  $-20\%$  and  $40\%$  for  $EA_1$  and  $-30\%$  and  $40\%$  for  $EA_2$ . The maximum and minimum values of the interval for a given  $\alpha$ -cut can be described for the two fuzzy variables as

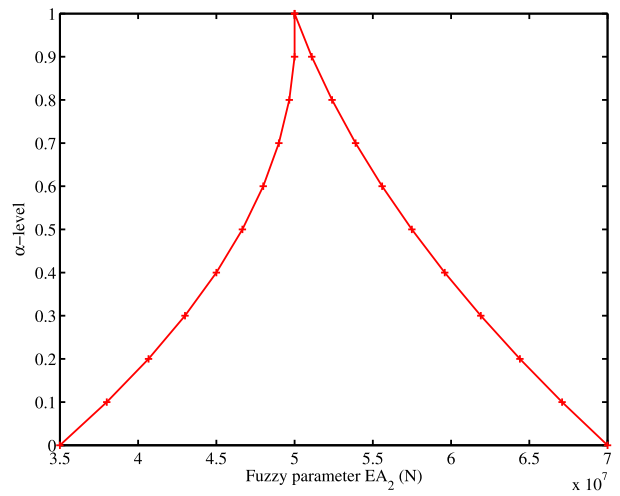
Table 7

Percentage error in the displacement at the end point of the rod computed using different order of Legendre polynomial based homogeneous chaos.

$\alpha$ -cut	1st order		2nd order		4th order	
	min	max	min	max	min	max
0.0	2.8522	2.4338	0.3426	0.2891	0.0039	0.0040
0.1	2.2891	1.9846	0.2471	0.2121	0.0023	0.0023
0.2	1.7931	1.5795	0.1719	0.1500	0.0013	0.0013
0.3	1.3618	1.2187	0.1141	0.1013	0.0007	0.0007
0.4	0.9930	0.9028	0.0713	0.0644	0.0003	0.0003
0.5	0.6848	0.6325	0.0410	0.0376	0.0001	0.0001
0.6	0.4354	0.4086	0.0208	0.0195	0.0000	0.0000
0.7	0.2435	0.2321	0.0087	0.0083	0.0000	0.0000
0.8	0.1076	0.1043	0.0026	0.0025	0.0000	0.0000
0.9	0.0268	0.0264	0.0003	0.0003	0.0000	0.0000
1.0	0.0000	0.0000	0.0000	0.0000	0.0000	0.0000



(a) Variation of  $AE_1$



(b) Variation of  $AE_2$

Fig. 7. Fuzzy description of the axial stiffness parameters  $AE_1$  and  $AE_2$  with nonlinear membership functions showing nonlinear variability of the intervals with  $\alpha$ . The crisp values are same as the previous case of linear membership functions, that is,  $\bar{EA}_1 = 20 \times 10^7$  N,  $\bar{EA}_2 = 5 \times 10^7$  N.

$$EA_{1_{\min}} = \bar{EA}_1(0.8 + 0.2\alpha^2) \quad \text{and} \quad EA_{1_{\max}} = \bar{EA}_1(1.4 - 0.2\alpha - 0.2\alpha^2) \quad (85)$$

$$EA_{2_{\min}} = \bar{EA}_2(0.7 + 0.6333\alpha - 0.3333\alpha^2) \quad \text{and} \quad EA_{2_{\max}} = \bar{EA}_2(1.4 - 0.6\alpha + 0.2\alpha^2) \quad (86)$$

For every  $\alpha$ -cut, we form the matrix  $\mathbf{K}_0^{(\alpha)}$  and  $\mathbf{K}_i^{(\alpha)}$  matrices for  $i = 1, 2$ . We solve Eq. (62) to obtain  $\mathbf{u}_j^{(\alpha)}$  for all the values of  $\alpha$ -cuts. Recall that for this problem, the dimension of Eq. (62) for the first-, second- and fourth-order approximations are 300, 600 and 1500 respectively. Results obtained from the proposed Legendre polynomial based approach is compared to the direct simulation results in Fig. 8. As expected, the fuzzy responses at both the points also vary nonlinearly with respect to different values of  $\alpha$ . Like the previous case, the results obtained by the second- and fourth-order chaos method are very accurate with respect to the direct simulation results. The percentage errors corresponding the responses at two points shown in Fig. 8, are given by Table 8 and Table 9 respectively. It can be observed that the error is very small up to 4th decimal place for higher values of  $\alpha$ -cut. For very low values of  $\alpha$ -cut and with the first-order approximation, one observes some noticeable errors. Overall, however, the errors are slightly greater compared to the linear case discussed in the previous subsection. From the point of view of accuracy necessary for engineering problems, second- or higher-order methods are acceptable for this problem.



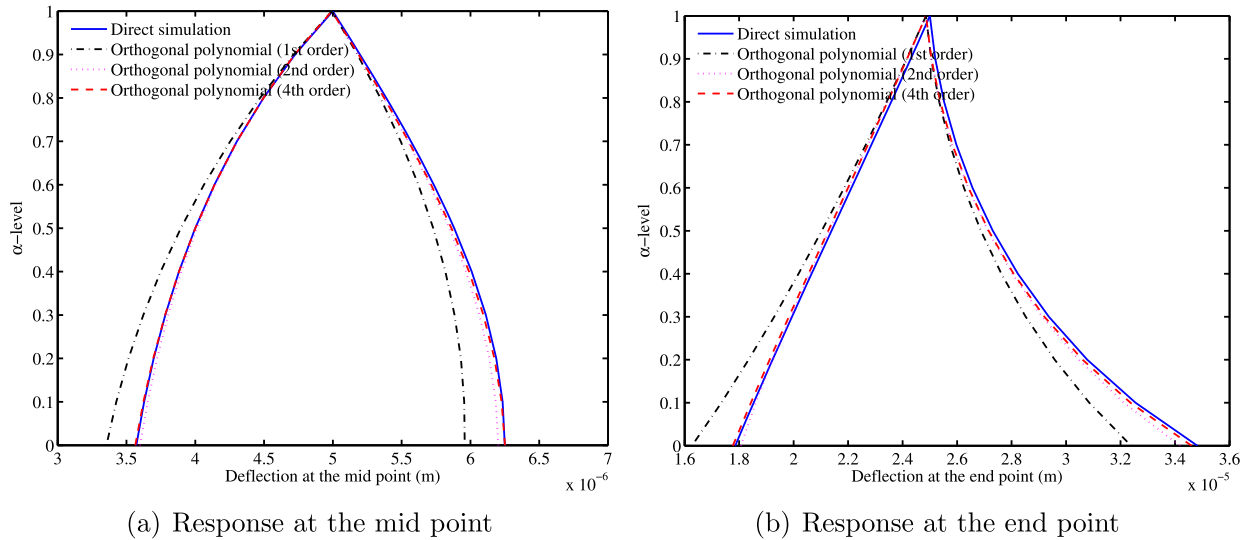


Fig. 9. Fuzzy description of the response of the rod at two points computed using different order of reduced Legendre polynomial based homogeneous chaos and direct simulation.

Table 10

Percentage error in the displacement at the mid point of the rod computed using different order of reduced Legendre polynomial based homogeneous chaos.

$\alpha$ -cut	1st order		2nd order		4th order	
	min	max	min	max	min	max
0.0	6.0835	4.6673	0.7706	0.7506	0.2069	0.0186
0.1	5.5763	4.4812	0.7282	0.8120	0.1418	0.1237
0.2	4.9473	4.1605	0.6519	0.8143	0.0867	0.2239
0.3	4.2213	3.7227	0.5499	0.7705	0.0424	0.2900
0.4	3.4321	3.1901	0.4326	0.6937	0.0097	0.3280
0.5	2.6215	2.5910	0.3110	0.5969	0.0102	0.3425
0.6	1.8381	1.9604	0.1954	0.4925	0.0158	0.3366
0.7	1.1364	1.3411	0.0932	0.3909	0.0055	0.3124
0.8	0.5760	0.7856	0.0072	0.2990	0.0227	0.2714
0.9	0.2211	0.3587	0.0666	0.2183	0.0709	0.2142
1.0	0.1411	0.1411	0.1411	0.1411	0.1411	0.1411

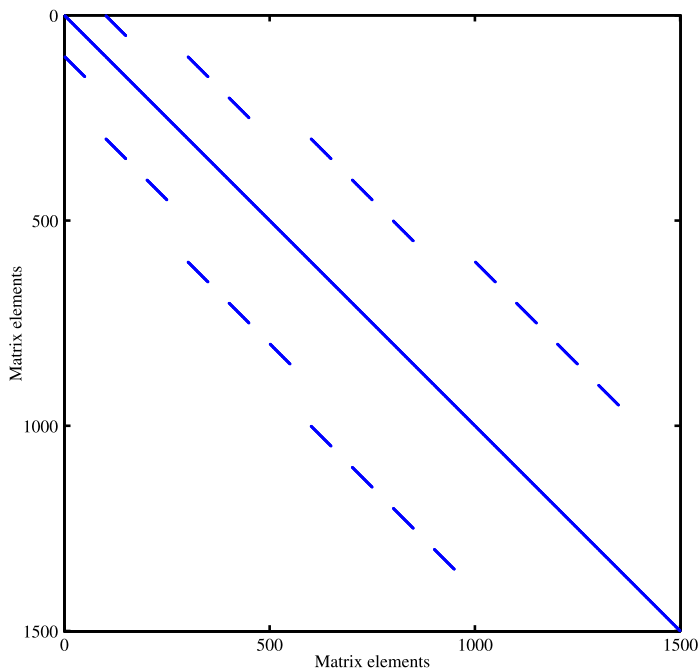
#### 5.4. Reduced approach

In this section we investigate the efficiency and accuracy of the reduced method proposed in Section 4.3. The finite element model of the system has  $n = 100$  degrees of freedom. For the reduced model, we are taking the first 20 eigenmodes so that  $p = 20$ . As a result, the dimension of the reduced set of equations in (75) becomes 60, 120 and 300 respectively for the first-, second- and fourth-order approximations. This amounts to a reduction of 80% of the original system in Eq. (62) which has dimensions of 300, 600 and 1500 for the corresponding approximations. The fuzzy description of the response of the rod at two points computed using different order of reduced Legendre polynomial based homogeneous chaos and direct simulation are shown in Fig. 9. Nonlinear membership functions, as considered in the previous subsection, are used as examples. The results follow a trend similar to the one in the previous examples, that is, acceptable accuracies are obtained except for the first-order approach. The corresponding error for the two points are shown in Tables 10, 11. The errors are relatively higher compared to the case with all the degrees of freedom discussed in the previous subsection. But considering that computational burden is about 80% less, this is an acceptable tradeoff. In Fig. 10 we show the structure of the matrices arising the Galerkin method for the full and reduced approaches for the fourth-order approximation. has dimension 1500 while the reduced matrix has dimension 300. In spite of this reduction, the accuracy of the numerical results are acceptable for this example.

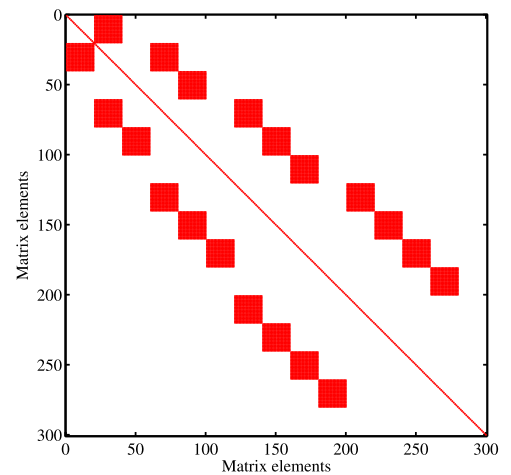
Table 11

Percentage error in the displacement at the end point of the rod computed using different order of reduced Legendre polynomial based homogeneous chaos.

$\alpha$ -cut	1st order		2nd order		4th order	
	min	max	min	max	min	max
0.0	8.9000	6.9922	1.1487	1.8390	0.4943	0.6087
0.1	6.3851	5.2183	0.4418	1.3315	0.5278	0.5731
0.2	4.5716	3.8881	0.0196	1.0202	0.5442	0.5596
0.3	3.2661	2.8904	0.2315	0.8303	0.5532	0.5553
0.4	2.3327	2.1439	0.3797	0.7147	0.5587	0.5544
0.5	1.6733	1.5893	0.4666	0.6441	0.5621	0.5546
0.6	1.2157	1.1833	0.5165	0.6010	0.5639	0.5549
0.7	0.9070	0.8950	0.5439	0.5755	0.5641	0.5551
0.8	0.7089	0.7027	0.5566	0.5620	0.5630	0.5555
0.9	0.5967	0.5926	0.5598	0.5571	0.5607	0.5562
1.0	0.5578	0.5578	0.5578	0.5578	0.5578	0.5578



(a) Matrix for the full method



(b) Matrix for the reduced method

Fig. 10. The structure of the matrices arising the Galerkin method for the full and reduced approaches for the fourth-order approximation. The full matrix has dimension 1500 while the reduced matrix has dimension 300.

## 6. Conclusions

Uncertainty propagation in complex systems with fuzzy variables is considered. An orthogonal function expansion approach in conjunction with Galerkin type error minimisation is proposed. This method has three major steps: (a) transformation of a fuzzy variable into a set of interval variables for different  $\alpha$ -cuts via the membership function, (b) transformation of interval variables into a standard interval variable between  $[-1, 1]$  for each  $\alpha$ -cut, and (c) projection of the response function in the basis of multivariate orthogonal Legendre polynomials in terms of the transformed standard interval variables. The coefficients associated with the basis functions are obtained using a Galerkin type of error minimisation. Depending on the number of bases retained in the series expansion, it is shown that various orders of approximation can be obtained. Closed-form expressions for the case of two fuzzy variables with up to fourth-order

approximations have been derived. The analytical technique can be extended to more variables with higher-order approximations, albeit with higher computational cost.

The method is first illustrated using scalar functions of multiple fuzzy variables. Good agreement with the results obtained from the direct numerical simulations was observed. A computational method is proposed for elliptic type fuzzy finite element problems, where the technique is generalised to vector valued functions with multiple fuzzy variables. For a given  $\alpha$ -cut, the stiffness matrix is expressed as a series involving standard interval variables and coefficient matrices. This novel representation significantly simplifies the problem of response prediction via the proposed multivariate orthogonal Legendre polynomials expansion technique. The coefficient vectors in the polynomial expansion are calculated from the solution of an extended set of linear algebraic equations. An eigenfunction based model reduction technique is proposed to obtain the coefficient vectors in an efficient way. A numerical example of axial deformation of a rod with fuzzy axial stiffness is considered to illustrate the proposed methods. Linear and nonlinear membership functions are used and the results are compared with direct numerical simulation results. The reduced approach proposed here is applied with a dimension reduction of 80%. Excellent accuracy has been observed for the second- and fourth-order approximations using the normal as well as the reduced approach.

The spectral method proposed in this paper can propagate fuzzy uncertainty in a mathematically rigorous and general manner similar to what is available for propagation of probabilistic uncertainty. The main computational cost involves the solution of an extended set of linear algebraic equations necessary to obtain the coefficients associated with the polynomial basis functions. Future research is necessary to develop computationally efficient methods to deal with this problem arising in systems with a large number of fuzzy variables.

## Acknowledgements

Financial support from The Royal Society of London through the Wolfson Research Merit award is gratefully acknowledged.

## References

- [1] O.C. Zienkiewicz, R.L. Taylor, *The Finite Element Method*, 4th edition, McGraw-Hill, London, 1991.
- [2] R. Ghanem, P. Spanos, *Stochastic Finite Elements: A Spectral Approach*, Springer-Verlag, New York, USA, 1991.
- [3] R. Chowdhury, S. Adhikari, High-dimensional model representation for stochastic finite element analysis, *Appl. Math. Model.* 34 (12) (2010) 3917–3932.
- [4] S. Adhikari, A reduced spectral function approach for the stochastic finite element analysis, *Comput. Methods Appl. Mech. Eng.* 200 (21–22) (2011) 1804–1821.
- [5] R.E. Moore, *Interval Analysis*, Prentice-Hall, Englewood Cliffs, NJ, USA, 1966.
- [6] Y.B. Haim, I. Elishakoff, *Convex Models of Uncertainty in Applied Mechanics*, Elsevier, Amsterdam, 1990.
- [7] L.A. Zadeh, Fuzzy sets, *Inf. Control* 8 (3) (1965) 338–353.
- [8] D. Moens, D. Vandepitte, Recent advances in non-probabilistic approaches for non-deterministic dynamic finite element analysis, *Arch. Comput. Methods Eng.* 13 (3) (2006) 389–464.
- [9] B. Mace, K. Worden, G. Manson, Uncertainty in structural dynamics, *J. Sound Vib.* 288 (3) (2005) 423–429.
- [10] D. Moens, M. Hanss, Non-probabilistic finite element analysis for parametric uncertainty treatment in applied mechanics: Recent advances, *Finite Elem. Anal. Des.* 47 (1) (2011) 4–16.
- [11] D. Dubois, H. Prade, *Possibility Theory: An Approach to Computerized Processing of Uncertainty*, vol. 2, Plenum Press, New York, 1988.
- [12] D. Dubois, H. Nguyen, H. Prade, Possibility theory, probability and fuzzy sets misunderstandings, bridges and gaps, in: *Fundamentals of Fuzzy Sets*, Springer, 2000, pp. 343–438.
- [13] D. Degrauwe, G. Lombaert, G.D. Roeck, Improving interval analysis in finite element calculations by means of affine arithmetic, *Comput. Struct.* 88 (3–4) (2010) 247–254.
- [14] Z. Qiu, X. Wang, M. Friswell, Eigenvalue bounds of structures with uncertain-but-bounded parameters, *J. Sound Vib.* 282 (1–2) (2005) 297–312.
- [15] B. Lallemand, G. Plessis, T. Tison, P. Level, Neumann expansion for fuzzy finite element analysis, *Eng. Comput.* 16 (5) (1999) 572–583.
- [16] M. Hanss, The transformation method for the simulation and analysis of systems with uncertain parameters, *Fuzzy Sets Syst.* 130 (3) (2002) 277–289.
- [17] M. De Munck, D. Moens, W. Desmet, D. Vandepitte, A response surface based optimisation algorithm for the calculation of fuzzy envelope FRFs of models with uncertain properties, *Comput. Struct.* 86 (10) (2008) 1080–1092.
- [18] D. Moens, D. Vandepitte, A fuzzy finite element procedure for the calculation of uncertain frequency-response functions of damped structures: Part I. Procedure, in: *Meeting on Uncertainty in Structural Dynamics*, Southampton, England 2003, *J. Sound Vib.* 288 (3) (2005) 431–462.
- [19] F. Massa, T. Tison, B. Lallemand, Fuzzy modal analysis: Prediction of experimental behaviours, *J. Sound Vib.* 322 (1–2) (2009) 135–154.
- [20] F. Massa, K. Ruffin, T. Tison, B. Lallemand, A complete method for efficient fuzzy modal analysis, *J. Sound Vib.* 309 (1–2) (2008) 63–85.

- [21] F. Massa, B. Lallemand, T. Tison, P. Level, Fuzzy eigensolutions of mechanical structures, *Eng. Comput.* 21 (1) (2004) 66–77.
- [22] G. Plessis, B. Lallemand, T. Tison, P. Level, Fuzzy modal parameters, *J. Sound Vib.* 233 (5) (2000) 797–812.
- [23] S.S. Rao, K.K. Annamdas, Evidence-based fuzzy approach for the safety analysis of uncertain systems, *AIAA J.* 46 (9) (2008) 2383–2387.
- [24] L. Farkas, D. Moens, D. Vandepitte, W. Desmet, Fuzzy finite element analysis based on reanalysis technique, *Struct. Saf.* 32 (6) (2010) 442–448.
- [25] S.S. Rao, Q. Liu, Fuzzy optimal controller design with application to fuzzy modeled structures, *AIAA J.* 46 (7) (2008) 1864–1873.
- [26] S. Rao, L. Cao, Fuzzy boundary element method for the analysis of imprecisely defined systems, *AIAA J.* 39 (9) (2001) 1788–1797.
- [27] R. Chowdhury, S. Adhikari, Fuzzy parametric uncertainty analysis of linear dynamical systems: A surrogate modeling approach, *Mech. Syst. Signal Process.* 32 (10) (2012) 5–17.
- [28] D. Xiu, G.E. Karniadakis, The Wiener–Askey polynomial chaos for stochastic differential equations, *SIAM J. Sci. Comput.* 24 (2) (2002) 619–644.
- [29] N. Wiener, The homogeneous chaos, *Am. J. Math.* 60 (897) (1938) 936.
- [30] G. Maglaras, E. Nikolaidis, R.T. Haftka, H.H. Cudney, Analytical-experimental comparison of probabilistic methods and fuzzy set based methods for designing under uncertainty, *Struct. Multidiscip. Optim.* 13 (2) (1997) 69–80.
- [31] S. Chen, E. Nikolaidis, H.H. Cudney, R. Rosca, R.T. Haftka, Comparison of probabilistic and fuzzy set methods for designing under uncertainty, *American Institute of Aeronautics and Astronautics*, 1999, pp. 99–1579.
- [32] M. Hanss, *Applied Fuzzy Arithmetic: An Introduction with Engineering Applications*, Springer, 2005.
- [33] H.J. Zimmermann, *Fuzzy Set Theory and Its Applications*, Springer, 2001.
- [34] D. Dubois, H. Prade, *Fuzzy Sets and Systems: Theory and Applications*, *Mathematics in Science & Engineering*, vol. 144, Academic Press, 1980.
- [35] D. Dubois, H. Prade, The three semantics of fuzzy sets, *Fuzzy Sets Syst.* 90 (2) (1997) 141–150.
- [36] L.A. Zadeh, Fuzzy sets as a basis for a theory of possibility, *Fuzzy Sets Syst.* 1 (1) (1978) 3–28.
- [37] D. Dubois, Possibility theory and statistical reasoning, *Comput. Stat. Data Anal.* 51 (1) (2006) 47–69.
- [38] S.M. Baas, H. Kwakernaak, Rating and ranking of multiple-aspect alternatives using fuzzy sets, *Automatica* 13 (1) (1977) 47–58.
- [39] D. Degrauwe, G. De Roeck, G. Lombaert, Uncertainty quantification in the damage assessment of a cable-stayed bridge by means of fuzzy numbers, *Comput. Struct.* 87 (17–18) (2009) 1077–1084.
- [40] L.A. Zadeh, The concept of a linguistic variable and its application to approximate reasoning—I, *Inf. Sci.* 8 (3) (1975) 199–249.
- [41] H.T. Nguyen, A note on the extension principle for fuzzy sets, *J. Math. Anal. Appl.* 64 (2) (1978) 369–380.
- [42] A. Neumaier, *Interval Methods for Systems of Equations*, vol. 37, Cambridge University Press, 1991.
- [43] M. Abramowitz, I.A. Stegun, *Handbook of Mathematical Functions, with Formulas, Graphs, and Mathematical Tables*, Dover Publications, Inc., New York, USA, 1965.
- [44] S. Berkowitz, F.J. Garner, The calculation of multidimensional Hermite polynomials and Gram–Charlie coefficients, *Math. Comput.* 24 (11) (1970) 537–545.
- [45] R. Grandhi, L. Wang, Higher-order failure probability calculation using nonlinear approximations, *Comput. Methods Appl. Mech. Eng.* 168 (1–4) (1999) 185–206.
- [46] L.C.W. Dixon, G.P. Szego, *The Optimization Problem: An Introduction*, North-Holland, New York, 1978.
- [47] J.H. Wilkinson, *The Algebraic Eigenvalue Problem*, Oxford University Press, Oxford, UK, 1988.
- [48] V. Lenaerts, G. Kerschen, J.C. Golinval, Physical interpretation of the proper orthogonal modes using the singular value decomposition, *J. Sound Vib.* 249 (5) (2002) 849–865.